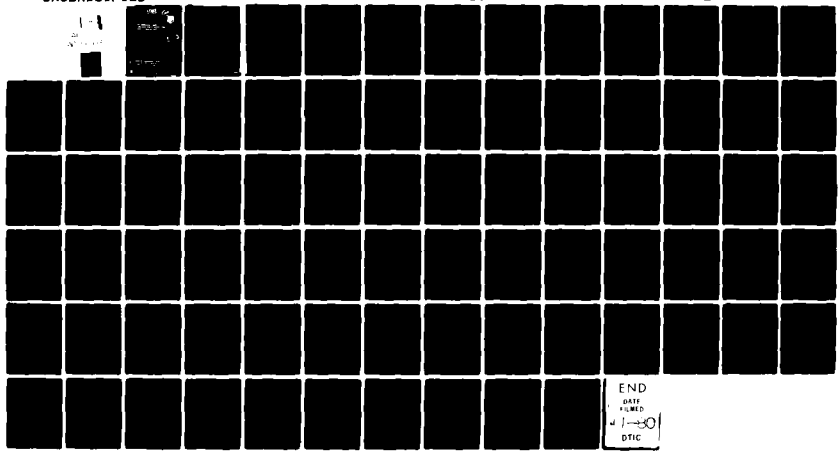


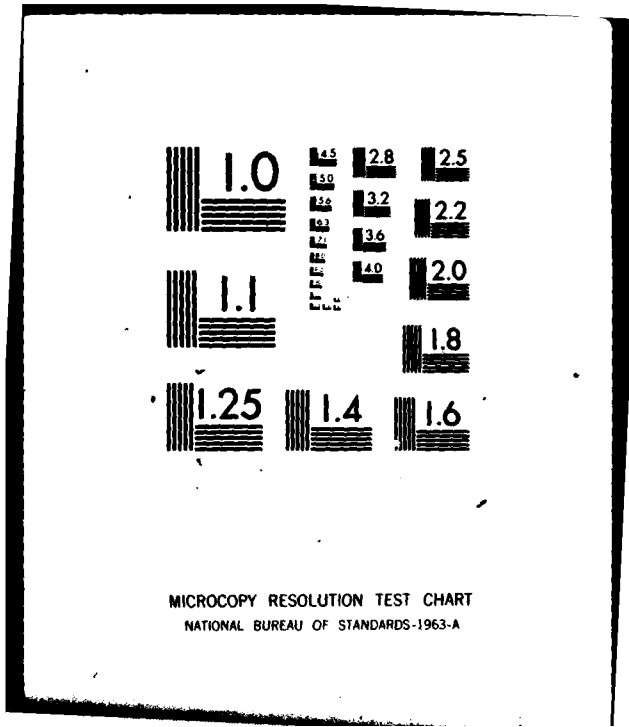
AD-A089 703 SYRACUSE UNIV NY DEPT OF ELECTRICAL AND COMPUTER EN--ETC F/G 20/3
AN IMPROVED E-FIELD SOLUTION FOR A CONDUCTING BODY OF REVOLUTIO--ETC(U)
JUN 80 J R MAUTZ, R F HARRINGTON F30602-79-C-0011

UNCLASSIFIED

RADC-TR-80-194

NL





MICROCOPY RESOLUTION TEST CHART
NATIONAL BUREAU OF STANDARDS-1963-A

AD A089703

UNCLASSIFIED
DATE 01-11-2001 BY [illegible]

[REDACTED]

APR 19 1964

[REDACTED]

[Faint, illegible text]

[Faint, illegible text]

[Faint, illegible text]
JUNE 2, 1979
ATTORNEY GENERAL, STATE OF TEXAS

[Faint, illegible text]

[Faint, illegible text]

[Faint, illegible text]

[Faint, illegible text]

[Faint, illegible text]

[Faint, illegible text]

[Faint, illegible text]

UNCLASSIFIED

SECURITY CLASSIFICATION OF THIS PAGE (When Data Entered)

19 REPORT DOCUMENTATION PAGE		READ INSTRUCTIONS BEFORE COMPLETING FORM
1. REPORT NUMBER RADC/TR-80-194	2. GOVT ACCESSION NO. AD-A089	3. RECIPIENT'S CATALOG NUMBER 703
4. TITLE (and Subtitle) AN IMPROVED E-FIELD SOLUTION FOR A CONDUCTING BODY OF REVOLUTION		5. TYPE OF REPORT & PERIOD COVERED Phase Report
7. AUTHOR(s) Joseph R. Mautz Roger F. Harrington		6. PERFORMING ORG. REPORT NUMBER N/A
9. PERFORMING ORGANIZATION NAME AND ADDRESS Syracuse University Department of Electrical and Computer Engineering, Syracuse NY 13210		8. CONTRACT OR GRANT NUMBER(s) F30602-79-C-0011
11. CONTROLLING OFFICE NAME AND ADDRESS Rome Air Development Center (RBCT) Griffiss AFB NY 13441		10. PROGRAM ELEMENT, PROJECT, TASK AREA & WORK UNIT NUMBERS 62702F 23300317
14. MONITORING AGENCY NAME & ADDRESS (if different from Controlling Office) Same		12. REPORT DATE June 1980
		13. NUMBER OF PAGES 78
		15. SECURITY CLASS. (of this report) UNCLASSIFIED
		15a. DECLASSIFICATION/DOWNGRADING SCHEDULE N/A
16. DISTRIBUTION STATEMENT (of this Report) Approved for public release; distribution unlimited.		
17. DISTRIBUTION STATEMENT (of the abstract entered in Block 20, if different from Report) Same		
18. SUPPLEMENTARY NOTES RADC Project Engineer: Roy F. Stratton (RBCT)		
19. KEY WORDS (Continue on reverse side if necessary and identify by block number) Body of revolution Computer program E-Field solution Method of moments		
20. ABSTRACT (Continue on reverse side if necessary and identify by block number) The electric field integro-differential equation for electromagnetic scattering from a perfectly conducting body of revolution is solved by the method of moments. A numerical solution is obtained by means of a computer program which is described and listed. This computer program is designed to handle oblique plane wave incidence efficiently. Spatial staggering of expansion functions for the orthogonal components of the induced current is known to give good accuracy		

H16737

406737 xlt

UNCLASSIFIED

SECURITY CLASSIFICATION OF THIS PAGE(When Data Entered)

Item 20 (Cont'd)

when the body of revolution has edges. By means of triangle and pulse expansion functions, this spatial staggering is achieved without the use of shifted source segments. The present computer program is highly competitive with other available programs as concerns storage, execution time, and accuracy.

Accession For	
BTIS GEM-I	<input checked="" type="checkbox"/>
DDC TAB	<input type="checkbox"/>
Unannounced	<input type="checkbox"/>
Justification	
By _____	
Distribution/	
Availability	
Dist.	Available for special
A	

UNCLASSIFIED

SECURITY CLASSIFICATION OF THIS PAGE(When Data Entered)

CONTENTS

	Page
PART ONE - SOLUTION PROCEDURE AND NUMERICAL RESULTS	
I. INTRODUCTION-----	1
II. METHOD OF MOMENTS SOLUTION-----	4
III. EVALUATION OF THE MOMENT MATRIX-----	9
IV. EVALUATION OF THE PLANE WAVE EXCITATION VECTOR-----	27
V. NUMERICAL RESULTS-----	32
 PART TWO - COMPUTER PROGRAM	
I. INTRODUCTION-----	41
II. THE SUBROUTINE ZMAT-----	43
III. THE FUNCTION BLOG-----	56
IV. THE SUBROUTINE PLANE-----	57
V. THE SUBROUTINES DECOMP AND SOLVE-----	63
VI. THE MAIN PROGRAM-----	65
 REFERENCES-----	 70

LIST OF TABLES

	Page
Table 1. Third to eleventh arguments of ZMAT-----	44
Table 2. Storage of matrix elements in Z'-----	50
Table 3. Fourth to ninth arguments of PLANE-----	58

LIST OF FIGURES

	Page
Fig. 1. Triangle function $T_j(t)$ -----	5
Fig. 2. Pulse function $P_j(t)$ -----	5
Fig. 3. Pulse doublet $\frac{d}{dt} T_j(t)$ -----	5
Fig. 4. Electric current for axial incidence on a circular disk of radius 0.25λ , $t = 0$ at center-----	35
Fig. 5. Electric current for axial incidence on a circular disk of radius 1.5λ , $t = 0$ at center-----	35
Fig. 6. Electric current for axial incidence on a circular washer of inside radius 0.4λ and outside radius 1.2λ , $t = 0$ at inside edge-----	36
Fig. 7. Electric current on a cone-sphere of cone angle 20° and sphere radius 0.2λ , incidence on sphere-----	37
Fig. 8. Electric current on a cone-sphere of cone angle 20° and sphere radius 0.2λ , incidence on tip-----	37
Fig. 9. Electric current on an open-ended cylinder of radius $\lambda/(2\pi)$ and length λ , incidence on $t = 0$ -----	39
Fig. 10. Electric current on a spherical shell of radius 0.2λ with axially symmetric aperture, edge at $t = 0.471\lambda$, incidence on aperture-----	39

PART ONE

SOLUTION PROCEDURE AND NUMERICAL RESULTS

I. INTRODUCTION

The purpose of this report is to develop an efficient numerical solution to the E-field integro-differential equation for electromagnetic excitation of a perfectly conducting body of revolution. This numerical solution is obtained by applying the method of moments to the E-field equation. The E-field equation states that the tangential component of the total electric field is zero on the surface S of the body of revolution.

The problem is stated in Section II of [1] and the solution is similar to that in Section IV of [1]. Except where otherwise indicated, the notation is the same as in [1]. Equation numbers drawn from [1] are preceded by 1-. For instance, (1-40) denotes equation (40) of reference [1].

The following differences exist between the present solution and that in [1]. In the present solution, the approximation to the generating curve of the body of revolution consists of half as many straight line segments as in [1]. Otherwise, the t directed expansion functions are the same as those in [1]. However, for ϕ directed expansion functions, the pulses used in [2] are adopted. Here, t is the arc length along the generating curve and ϕ is the azimuthal angle. The testing functions are the complex conjugates of the expansion functions. For calculation of the elements of the moment matrix, each integral with respect to t' over each straight line segment is evaluated by using n_t -point Gaussian quadrature

and each integral with respect to t over each straight line segment is approximated by sampling at the midpoint of the line segment. Although t and t' are both arc lengths along the generating curve, t denotes integration over a testing function and t' denotes integration over an expansion function. The former integration is called a field integration, the latter a source integration. As in [1], n_ϕ -point Gaussian quadrature is used for the integration with respect to ϕ . However, the method [3] of eliminating the singularity is used to fortify the Gaussian quadrature integrations with respect to t' and ϕ whenever the source segment is sufficiently close to the field point. For calculation of the elements of the excitation vector, n_T -point Gaussian quadrature is used for the t integration.

With regard to ϕ directed testing, calculation of the moment matrix by sampling the t integrand at the center of each straight line segment is equivalent to point matching. However, for t directed testing, this calculation can not be viewed as simple point matching because each t directed testing function extends over two intervals and therefore must be represented by two Dirac delta functions instead of one. Furthermore, the electric charge associated with each t directed testing function is also represented by two Dirac delta functions.

The method of solution formulated in Part One of this report is implemented by the computer program described and listed in Part Two. The present computer program takes almost twice as long to compile as that in [1]. However, for axial incidence and for moment matrices of roughly the same order, the present program with $n_t = n_T = 2$ and $n_\phi = 20$ executes almost as fast as that in [1] with $N_\phi = 20$. For moment matrices of the

same order, the present computer program probably executes faster than that in [2] because the one in [2] uses twice as many source segments and twice as many field points. For oblique incidence, several moment matrices are required. The computer program in [1] calculates the moment matrices one by one, that is, each moment matrix is calculated from scratch. However, the present computer program takes advantage of the fact that some intermediate calculations are common to all the moment matrices. Hence, if there is room enough to store all the moment matrices simultaneously, the present computer program should execute much faster for oblique incidence. Results obtained from the present computer program are generally more accurate than those obtained from [1], especially for bodies of revolution with edges.

II. METHOD OF MOMENTS SOLUTION

The boundary condition that the tangential component of the total electric field is zero on S is expressed by (1-40) and supporting equations (1-41)-(1-43). Following the method of moments, we approximate the electric current \underline{J} on S by

$$\underline{J} = \sum_{n,j} (I_{nj}^t \underline{J}_{nj}^t + I_{nj}^\phi \underline{J}_{nj}^\phi) \quad (1)$$

and substitute this \underline{J} into (1-41). In (1), \underline{J}_{nj}^t and \underline{J}_{nj}^ϕ are known expansion functions and I_{nj}^t and I_{nj}^ϕ are unknown coefficients to be determined.

The expansion functions \underline{J}_{nj}^t and \underline{J}_{nj}^ϕ are defined by

$$\underline{J}_{nj}^t = \underline{u}_t \frac{T_j(t)}{\rho} e^{jn\phi} \quad \begin{array}{l} j = 1, 2, \dots, P-2 \\ n = 0, \pm 1, \pm 2, \dots \end{array} \quad (2)$$

$$\underline{J}_{nj}^\phi = \underline{u}_\phi \frac{P_j(t)}{\rho_j} e^{jn\phi} \quad \begin{array}{l} j = 1, 2, \dots, P-1 \\ n = 0, \pm 1, \pm 2, \dots \end{array} \quad (3)$$

where \underline{u}_t and \underline{u}_ϕ are unit vectors in the t and ϕ directions, respectively. The j which appears in the argument of the exponential in (2) and (3) is not to be confused with the j which appears elsewhere in (2) and (3). The former j is $\sqrt{-1}$ and the latter j is the subscript which goes from 1 to either $P-2$ or $P-1$. The function $T_j(t)$ is the triangle function shown in Fig. 1 and ρ is the distance from the axis of the body of revolution. The function $P_j(t)$ is the pulse function shown in Fig. 2 and ρ_j is the value of ρ at $t = t_j$ where t_j is the center point of the domain of the pulse. The purpose of the scale factor $1/\rho_j$ in (3) is to give (3) the same dimension as (2), namely, 1/length. The pulse doublet $\frac{d}{dt} T_j(t)$ in Fig. 3 is

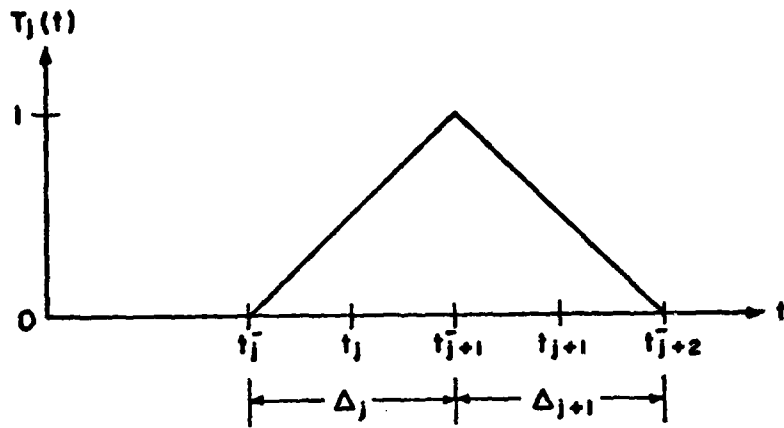


Fig. 1. Triangle function $T_j(t)$.

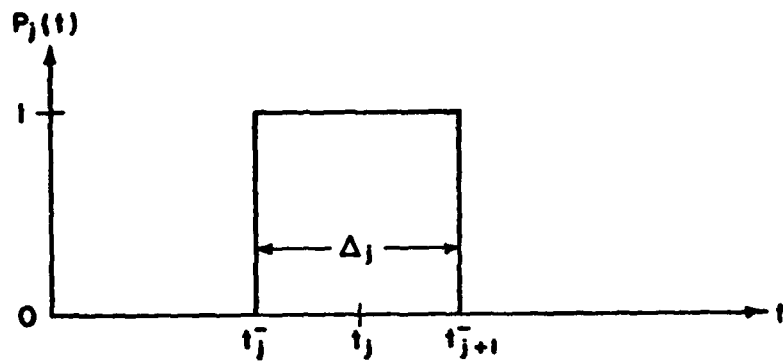


Fig. 2. Pulse function $P_j(t)$.

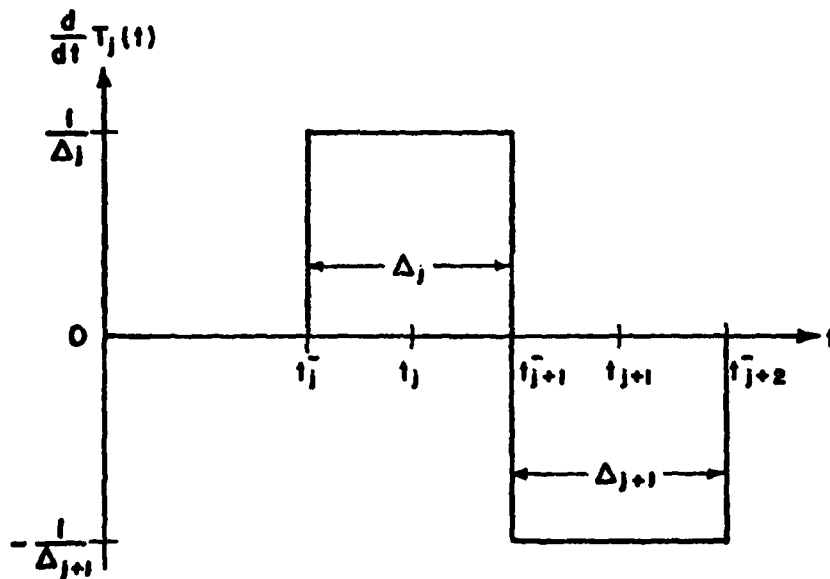


Fig. 3. Pulse doublet $\frac{d}{dt} T_j(t)$.

used later on in the method of moments solution. In Figs. 1, 2, and 3, t is the arc length along the generating curve. It is assumed that the generating curve consists of $P-1$ straight line segments where P is an odd integer greater than or equal to 3. The j th such segment extends from t_j^- to t_{j+1}^- . Its length is Δ_j . The expansion functions (2) and (3) are especially appropriate if the body of revolution is an infinitely thin perfectly conducting surface with edges at both ends of the generating curve. This is true because the t directed electric current is supposed to approach zero at an edge whereas the ϕ directed electric current might grow large there [4].

Testing functions W_{ni}^t and W_{ni}^ϕ are defined by

$$\frac{W_{ni}^t}{\rho} = \frac{u_t}{\rho} \frac{T_i(t)}{\rho} e^{-jn\phi} \quad \begin{array}{l} i = 1, 2, \dots, P-2 \\ n = 0, \underline{+1}, \underline{+2}, \dots \end{array} \quad (4)$$

$$\frac{W_{ni}^\phi}{\rho_i} = \frac{u_\phi}{\rho_i} \frac{P_i(t)}{\rho_i} e^{-jn\phi} \quad \begin{array}{l} i = 1, 2, \dots, P-1 \\ n = 0, \underline{+1}, \underline{+2}, \dots \end{array} \quad (5)$$

After substitution of (1) into (1-41), the dot product of (1-41) is taken with each testing function. These dot products are then integrated over S . As can be derived by retracing the development (1-40)-(1-65) with (1-46) and (1-47) replaced by (2)-(5), the resulting matrix equation is

$$\begin{bmatrix} Z_n^{tt} & Z_n^{t\phi} \\ Z_n^{\phi t} & Z_n^{\phi\phi} \end{bmatrix} \begin{bmatrix} \vec{I}_n^t \\ \vec{I}_n^\phi \end{bmatrix} = \begin{bmatrix} \vec{V}_n^t \\ \vec{V}_n^\phi \end{bmatrix}, \quad n = 0, \underline{+1}, \underline{+2}, \dots \quad (6)$$

where the Z_n 's are submatrices and the \vec{I}_n 's and \vec{V}_n 's are column vectors.

The matrix of the Z_n 's on the left-hand side of (6) is a square matrix called the moment matrix. The column vector on the right-hand side of (6) is called the excitation vector. The j th element of \vec{I}_n^t is I_{nj}^t and that of \vec{I}_n^ϕ is I_{nj}^ϕ . The i th elements of \vec{V}_n^t and \vec{V}_n^ϕ are given by

$$V_{ni}^t = \frac{1}{\eta} \iint_S \underline{W}_{ni}^t \cdot \underline{E}^i dS, \quad i = 1, 2, \dots, P-2 \quad (7)$$

$$V_{ni}^\phi = \frac{1}{\eta} \iint_S \underline{W}_{ni}^\phi \cdot \underline{E}^i dS, \quad i = 1, 2, \dots, P-1 \quad (8)$$

where η is the intrinsic impedance and \underline{E}^i is the incident electric field. The ij th elements of the Z_n 's are given by

$$(Z_n^{tt})_{ij} = j \int_{t_i^-}^{t_{i+2}^-} dt \int_{t_j^-}^{t_{j+2}^-} dt' \{k^2 T_i(t) T_j(t') (G_5 \sin v \sin v' + G_7 \cos v \cos v') - G_7 \frac{d}{dt} T_i(t) \frac{d}{dt'} T_j(t')\} \quad (9)$$

$$(Z_n^{\phi t})_{ij} = -\frac{1}{\rho_i} \int_{t_i^-}^{t_{i+1}^-} dt P_i(t) \int_{t_j^-}^{t_{j+2}^-} dt' (k^2 \rho' T_j(t') G_6 \sin v' + n G_7 \frac{d}{dt'} T_j(t')) \quad (10)$$

$$(Z_n^{t\phi})_{ij} = \frac{1}{\rho_j} \int_{t_i^-}^{t_{i+2}^-} dt \int_{t_j^-}^{t_{j+1}^-} dt' P_j(t') (k^2 \rho' T_i(t) G_6 \sin v + n G_7 \frac{d}{dt} T_i(t)) \quad (11)$$

$$(Z_n^{\phi\phi})_{ij} = \frac{j}{\rho_i \rho_j} \int_{t_i^-}^{t_{i+1}^-} dt P_i(t) \int_{t_j^-}^{t_{j+1}^-} dt' P_j(t') (k^2 \rho \rho' G_5 - n^2 G_7) \quad (12)$$

where

$$G_7 = G_4 + G_5 \quad (13)$$

$$G_4 = 2 \int_0^{\pi} d\phi \frac{e^{-jkR}}{kR} \sin^2\left(\frac{\phi}{2}\right) \cos(n\phi) \quad (14)$$

$$G_5 = \int_0^{\pi} d\phi \frac{e^{-jkR}}{kR} \cos \phi \cos(n\phi) \quad (15)$$

$$G_6 = \int_0^{\pi} d\phi \frac{e^{-jkR}}{kR} \sin \phi \sin(n\phi) \quad (16)$$

$$R = \sqrt{(\rho' - \rho)^2 + (z' - z)^2 + 4\rho\rho' \sin^2\left(\frac{\phi}{2}\right)} \quad (17)$$

Here, k is the propagation constant, ρ is the distance from the axis of the body of revolution, z is the rectangular coordinate along this axis, and v is the angle that the tangent to the generating curve makes with the z axis. The angle v is positive if ρ increases with t and negative otherwise. The parameters ρ , z , and v depend on t . Their counterparts ρ' , z' , and v' depend on t' . The ranges of values of i and j in (9)-(12) are such that the regions of integration therein move from one end of the generating curve to the other end. It is understood that $n = 0, \pm 1, \pm 2, \dots$ in (7)-(16).

Note that the quantity G_4 defined by (14) is different from that defined by (1-62). The trigonometric identity

$$1 = 2 \sin^2\left(\frac{\phi}{2}\right) + \cos \phi \quad (18)$$

was used to express (1-62) as the sum of (14) and (15). Expression (14) is more suitable for computation than (1-62) because the integrand in (14) is always finite.

III. EVALUATION OF THE MOMENT MATRIX

One by one evaluation of the elements (9)-(12) of the moment matrix is inefficient because of the overlapping regions of integration. For instance, both $(Z_n^{tt})_{i-1,j}$ and $(Z_n^{tt})_{ij}$ contain integrals with respect to t over the i th segment (t_i^-, t_{i+1}^-) . If $(Z_n^{tt})_{i-1,j}$ and $(Z_n^{tt})_{ij}$ are calculated one after the other, these integrals must either be stored or calculated twice.

In this report, the contributions to (9)-(12) are accounted for by regions of integration rather than by matrix elements. Consider the contributions due to the 2-dimensional region of integration

$$\begin{aligned} t_p^- &\leq t \leq t_{p+1}^- \\ t_q^- &\leq t' \leq t_{q+1}^- \end{aligned}$$

This region of integration is called A_{pq} . Integrations in (9)-(12) are carried out over A_{pq} for $\{i=p, j=q\}$ or possibly $\{i=p-1, j=q\}$, $\{i=p, j=q-1\}$ and $\{i=p-1, j=q-1\}$.

For all other values of i and j , no region of integration in (9)-(12) intersects A_{pq} . Setting $\{i=p-1, j=q-1\}$, $\{i=p, j=q-1\}$, $\{i=p-1, j=q\}$, and $\{i=p, j=q\}$ successively in (9)-(12) and counting only the region of integration A_{pq} , we obtain

$$(Z_n^{*tt})_{ij} = j \int_{t_p^-}^{t_{p+1}^-} dt \int_{t_q^-}^{t_{q+1}^-} dt' \{k^2 T_i(t) T_j(t') (G_5 \sin v \sin v' + G_7 \cos v \cos v') - G_7 \frac{d}{dt} T_i(t) \frac{d}{dt'} T_j(t')\} \quad (19)$$

$$(Z_n^{*\phi t})_{pj} = -\frac{1}{\rho_p} \int_{t_p^-}^{t_{p+1}^-} dt P_p(t) \int_{t_q^-}^{t_{q+1}^-} dt' (k^2 \rho T_j(t') G_6 \sin v' + n G_7 \frac{d}{dt'} T_j(t')) \quad (20)$$

$$(Z_n^{*t\phi})_{iq} = \frac{1}{\rho_q} \int_{t_p^-}^{t_{p+1}^-} dt \int_{t_q^-}^{t_{q+1}^-} dt' P_q(t') (k^2 \rho' T_i(t) G_6 \sin v + n G_7 \frac{d}{dt} T_i(t)) \quad (21)$$

$$(Z_n^{\phi\phi})_{pq} = \frac{j}{\rho_p \rho_q} \int_{t_p^-}^{t_{p+1}^-} dt P_p(t) \int_{t_q^-}^{t_{q+1}^-} dt' P_q(t') (k^2 \rho \rho' G_5 - n^2 G_7) \quad (22)$$

In (19) and (21),

$$i = p-1, p$$

$$i \neq 0 \quad (23)$$

$$i \neq P-1$$

In (19) and (20),

$$j = q-1, q$$

$$j \neq 0 \quad (24)$$

$$j \neq P-1$$

The asterisk (*) on the left-hand sides of (19)-(21) denotes the contribution due to integration over the region A_{pq} . Note that (22) is (12) with ij replaced by pq . Because (12) has no overlapping regions of integration, it is not affected by the change from calculation by matrix elements to calculation by regions of integration.

Next, each integral with respect to t in (19)-(22) is evaluated by using the approximation

$$\int_{t_p^-}^{t_{p+1}^-} f(t) dt = f(t_p) \Delta_p \quad (25)$$

where $f(t)$ is the relevant integrand and, as indicated in Figs. 1, 2, and 3,

$$t_p = \frac{1}{2} (t_p^- + t_{p+1}^-) \quad (26)$$

$$\Delta_p = t_{p+1}^- - t_p^- \quad (27)$$

Application of (25) to each integral with respect to t in (19)-(22)

gives

$$\begin{aligned} (Z_n^{*tt})_{ij} = j\Delta_p \int_{t_q^-}^{t_{q+1}^-} dt' \{ k^2 T_i(t_p) T_j(t') (G_5 \sin v_p \sin v' + G_7 \cos v_p \cos v') - \\ - G_7 \left[\frac{d}{dt} T_i(t) \right]_{t_p} \frac{d}{dt'} T_j(t') \} \quad (28) \end{aligned}$$

$$(Z_n^{*\phi t})_{pj} = -\Delta_p P_p(t_p) \int_{t_q^-}^{t_{q+1}^-} dt' (k^2 T_j(t') G_6 \sin v' + \frac{n}{\rho_p} G_7 \frac{d}{dt'} T_j(t')) \quad (29)$$

$$(Z_n^{*t\phi})_{iq} = \Delta_p \int_{t_q^-}^{t_{q+1}^-} dt' P_q(t') \left(\frac{k^2 \rho'}{\rho_q} T_i(t_p) G_6 \sin v_p + \frac{n}{\rho_q} G_7 \left[\frac{d}{dt} T_i(t) \right]_{t_p} \right) \quad (30)$$

$$(Z_n^{\phi\phi})_{pq} = j\Delta_p P_p(t_p) \int_{t_q^-}^{t_{q+1}^-} dt' P_q(t') \left(\frac{k^2 \rho'}{\rho_q} G_5 - \frac{n^2}{\rho_p \rho_q} G_7 \right) \quad (31)$$

where v_p is the value of v at $t = t_p$. Incidentally, $v = v_p$ for $t_p^- < t < t_{p+1}^-$ because the generating curve was assumed to be straight there. In (28)-(31), G_5 , G_6 , and G_7 are given, respectively, by (15), (16), and (13) with R replaced by R_p where

$$R_p = \sqrt{(\rho' - \rho_p)^2 + (z' - z_p)^2 + 4\rho_p \rho' \sin^2 \left(\frac{\phi}{2} \right)} \quad (32)$$

where z_p is the value of z at $t = t_p$. The range of values of i and j

in (28)-(30) is, as inherited from (19)-(21), given by (23) and (24).

Application of (25) is only one way to obtain (28)-(31). Another way to obtain (28)-(31) is by approximating the G's in (19)-(22) by their values at $t = t_p$. This amounts to immediate rather than consequential replacement of R by R_p in (14)-(16). A third way to obtain (28)-(31) is by substituting the approximation

$$T_i(t) \approx \frac{1}{2} (\Delta_i \delta(t-t_i) + \Delta_{i+1} \delta(t-t_{i+1})) \quad (33)$$

$$P_p(t) \approx \Delta_p \delta(t-t_p) \quad (34)$$

$$\frac{d}{dt} T_i(t) \approx \delta(t-t_i) - \delta(t-t_{i+1}) \quad (35)$$

into (19)-(22). Here, $\delta(t)$ is the Dirac delta function. The approximation (33) preserves the value of the surface integral of the t component of the t directed electric current (4) on the portion of S for which

$$t_p^- \leq t \leq t_{p+1}^-, \quad p = 1, 2, \dots, P-1$$

$$\phi_a \leq \phi \leq \phi_b$$

where ϕ_a and ϕ_b are arbitrary. Likewise, the approximations (34) and (35) do not alter the values of such surface integrals of the electric current (5) and the electric charge associated with either (4) or (5).

Equations (28)-(31) were obtained by using the testing functions (4) and (5) and invoking either the approximation (25) or the set of approximations (33)-(35). Can a set of effective testing functions be defined such that (28)-(31) can be obtained by using these functions and no auxiliary approximation? Testing functions could be defined by substituting (33)

and (34) into (4) and (5), but the approximation (35) would still be required in order to obtain (28)-(31). Unfortunately, the approximation (35) is not consistent with the approximation (33). Hence, it is not possible to trace (28)-(31) to effective testing functions.

The functions $P_q(t')$, $T_j(t')$, $\frac{d}{dt'} T_j(t')$, v' , and ρ' in (28)-(31) are given by

$$P_q(t') = 1 \quad (36)$$

$$T_j(t') = \frac{1}{2} + \frac{(-1)^{q-j}(t'-t_q)}{\Delta_q}, \quad j = q-1, q \quad (37)$$

$$\frac{d}{dt'} T_j(t') = \frac{(-1)^{q-j}}{\Delta_q}, \quad j = q-1, q \quad (38)$$

$$v' = v_q \quad (39)$$

$$\rho' = \rho_q + (t'-t_q) \sin v_q \quad (40)$$

for $t_q^- < t' < t_{q+1}^-$. Equations (36)-(38) can be obtained from Figs. 1, 2, and 3. Equations (39) and (40) are true because the generating curve is straight for $t_q^- < t' < t_{q+1}^-$. Replacement of j , q , and t' by i , p , and t_p in (36)-(38) gives

$$P_p(t_p) = 1 \quad (41)$$

$$T_i(t_p) = \frac{1}{2} \quad (42)$$

$$\left[\frac{d}{dt} T_i(t) \right]_{t_p} = \frac{(-1)^{p-i}}{\Delta_p} \quad (43)$$

Substitution of (36)-(43) into (28)-(31) yields

$$(Z_n^{*tt})_{ij} = j\Delta_p \int_{t_q^-}^{t_q^{q+1}^-} dt' \left\{ \frac{k^2}{4} \left(1 + \frac{(-1)^{q-j} 2(t'-t_q)}{\Delta_q} \right) (G_5 \sin v_p \sin v_q + G_7 \cos v_p \cos v_q) - \frac{(-1)^{p+q-i-j} G_7}{\Delta_p \Delta_q} \right\} \quad (44)$$

$$(Z_n^{*\phi t})_{pj} = -\Delta_p \int_{t_q^-}^{t_q^{q+1}^-} dt' \left(\frac{k^2}{2} \left(1 + \frac{(-1)^{q-j} 2(t'-t_q)}{\Delta_q} \right) G_6 \sin v_q + \frac{(-1)^{q-j} G_7}{\rho_p \Delta_q} \right) \quad (45)$$

$$(Z_n^{*\phi\phi})_{iq} = \Delta_p \int_{t_q^-}^{t_q^{q+1}^-} dt' \left(\frac{k^2}{2} \left(1 + \frac{(t'-t_q)}{\rho_q} \sin v_q \right) G_6 \sin v_p + \frac{(-1)^{p-i} G_7}{\rho_q \Delta_p} \right) \quad (46)$$

$$(Z_n^{\phi\phi})_{pq} = j\Delta_p \int_{t_q^-}^{t_q^{q+1}^-} dt' \left(k^2 \left(1 + \frac{(t'-t_q)}{\rho_q} \sin v_q \right) G_5 - \frac{n^2}{\rho_p \rho_q} G_7 \right) \quad (47)$$

Equations (42)-(45) are rewritten as

$$(Z_n^{*tt})_{ij} = \frac{j k^2 \Delta_p \Delta_q}{8} (G_{5a} \sin v_p \sin v_q + G_{7a} \cos v_p \cos v_q) + \frac{(-1)^{q-j} j k^2 \Delta_p \Delta_q}{8} (G_{5b} \sin v_p \sin v_q + G_{7b} \cos v_p \cos v_q) - (-1)^{p+q-i-j} \frac{1}{2} G_{7a} \quad (48)$$

$$(Z_n^{*\phi t})_{pj} = - \left(\frac{k^2 \Delta_p \Delta_q \sin v_q}{4} \right) G_{6a} - (-1)^{q-j} \left\{ \left(\frac{k^2 \Delta_p \Delta_q \sin v_q}{4} \right) G_{6b} + \frac{n \Delta_p}{2 \rho_p} G_{7a} \right\} \quad (49)$$

$$(Z_n^{*t\phi})_{iq} = \left(\frac{k^2 \Delta \Delta \sin v}{4 p q} \right) (G_{6a} + \frac{\Delta \sin v}{2 \rho_q} G_{6b}) + (-1)^{p-i} \left(\frac{n \Delta}{2 \rho_q} \right) G_{7a} \quad (50)$$

$$(Z_n^{\phi\phi})_{pq} = 2j \left\{ \left(\frac{k^2 \Delta \Delta}{4 p q} \right) (G_{5a} + \frac{\Delta \sin v}{2 \rho_q} G_{5b}) - \left(\frac{n \Delta}{2 \rho_q} \right) \left(\frac{n \Delta}{2 \rho_p} \right) G_{7a} \right\} \quad (51)$$

where i is either $p-1$ or p and j is either $q-1$ or q and where

$$G_{ma} = \frac{2}{\Delta_q} \int_{t_q}^{t_q^-} G_m dt' \quad (52)$$

$$m = 5, 6, 7$$

$$G_{mb} = \left(\frac{2}{\Delta_q} \right)^2 \int_{t_q}^{t_q^-} (t' - t_q) G_m dt' \quad (53)$$

Equation (13) is used to rewrite (52) and (53) as

$$G_{7a} = G_{4a} + G_{5a} \quad (54)$$

$$G_{7b} = G_{4b} + G_{5b} \quad (55)$$

$$G_{ma} = \left(\frac{2}{\Delta_q} \right) \int_{t_q}^{t_q^-} G_m (t' - t_q) dt' \quad (56)$$

$$m = 4, 5, 6$$

$$G_{mb} = \left(\frac{2}{\Delta_q} \right)^2 \int_{t_q}^{t_q^-} (t' - t_q) G_m (t' - t_q) dt' \quad (57)$$

The argument $(t' - t_q)$ supplied with G_m in (56) and (57) comes into play later on. Substitution of R_p for R in (14)-(16) produces

$$G_4(t' - t_q) = 2 \int_0^\pi d\phi \frac{e^{-jkR_p}}{kR_p} \sin^2\left(\frac{\phi}{2}\right) \cos(n\phi) \quad (58)$$

$$G_5(t' - t_q) = \int_0^\pi d\phi \frac{e^{-jkR_p}}{kR_p} \cos \phi \cos(n\phi) \quad (59)$$

$$G_6(t' - t_q) = \int_0^\pi d\phi \frac{e^{-jkR_p}}{kR_p} \sin \phi \sin(n\phi) \quad (60)$$

where R_p is given by (32). In (32), ρ' is given by (40) and z' by

$$z' = z_q + (t' - t_q) \cos v_q \quad (61)$$

Equation (61) is true because the portion of the generating curve for $t_q^- < t' < t_{q+1}^-$ is straight.

Evaluation of the integrals in (56) and (57) by means of an n_t -point Gaussian quadrature formula gives

$$G_{ma} = \sum_{\ell'=1}^{n_t} A_{\ell'}^{(n_t)} G_m\left(\frac{1}{2} \Delta_q x_{\ell'}^{(n_t)}\right) \quad m = 4, 5, 6 \quad (62)$$

$$G_{mb} = \sum_{\ell'=1}^{n_t} A_{\ell'}^{(n_t)} x_{\ell'}^{(n_t)} G_m\left(\frac{1}{2} \Delta_q x_{\ell'}^{(n_t)}\right) \quad (63)$$

where the abscissas $x_{\ell'}^{(n_t)}$ and weights $A_{\ell'}^{(n_t)}$ are tabulated in Appendix A of [5] for several values of n_t . Application of an n_ϕ -point Gaussian quadrature formula to the integrals in (58)-(60) and replacement of $(t' - t_q)$ by $\frac{1}{2} \Delta_q x_{\ell'}^{(n_t)}$ result in

$$G_4\left(\frac{1}{2} \Delta_q x_{\ell'}^{(n_t)}\right) = \pi \sum_{\ell=1}^{n_\phi} A_\ell^{(n_\phi)} \frac{e^{-jkR_{p\ell'\ell}}}{kR_{p\ell'\ell}} \sin^2\left(\frac{\phi_\ell}{2}\right) \cos(n\phi_\ell) \quad (64)$$

$$G_5\left(\frac{1}{2} \Delta_q x_{\ell'}^{(n_t)}\right) = \frac{\pi}{2} \sum_{\ell=1}^{n_\phi} A_\ell^{(n_\phi)} \frac{e^{-jkR_{p\ell'\ell}}}{kR_{p\ell'\ell}} \cos \phi_\ell \cos(n\phi_\ell) \quad (65)$$

$$G_6\left(\frac{1}{2} \Delta_q x_{\ell'}^{(n_t)}\right) = \frac{\pi}{2} \sum_{\ell=1}^{n_\phi} A_\ell^{(n_\phi)} \frac{e^{-jkR_{p\ell'\ell}}}{kR_{p\ell'\ell}} \sin \phi_\ell \sin(n\phi_\ell) \quad (66)$$

where

$$R_{p\ell'\ell} = \sqrt{(\rho' - \rho_p)^2 + (z' - z_p)^2 + 4\rho_p \rho' \sin^2\left(\frac{\phi_\ell}{2}\right)} \quad (67)$$

where

$$\rho' = \rho_q + \frac{1}{2} \Delta_q x_{\ell'}^{(n_t)} \sin v_q \quad (68)$$

$$z' = z_q + \frac{1}{2} \Delta_q x_{\ell'}^{(n_t)} \cos v_q \quad (69)$$

$$\phi_\ell = \frac{\pi}{2} (x_\ell^{(n_\phi)} + 1) \quad (70)$$

Calculated values of $G_m\left(\frac{1}{2} \Delta_q x_{\ell'}^{(n_t)}\right)$ from (64)-(66) are substituted into (62) and (63) in order to evaluate G_{ma} and G_{mb} . The resulting values of G_{ma} and G_{mb} are then substituted, either directly or through the intermediary equations (54) and (55), into formulas (48)-(51) for the elements of the moment matrix.

The values $n_t = 2$ and $n_\phi = 20$ are suggested whenever the field point is not close to the source segment. If the field point is close to the source segment, the method of eliminating the singularity [3] is used. Since double integrals are involved, three variations of the method are possible. These variations are called methods 1, 2, and 3. In method 1, elimination of the singularity is applied to the integration with respect to t' . In method 2, elimination of the singularity is applied to the integration with respect to ϕ . In method 3, it is applied to the double integral. In methods 1 and 2, the "singular part"

of the integrand is subtracted out, numerical integration of the resulting finite integrand is performed with respect to one of the variables, the integral (with respect to this variable) of the "singular part" is added, and then numerical integration with respect to the other variable is done. In method 3, the singular part of the integrand is subtracted out, numerical integration of the resulting finite integrand is performed with respect to both variables, and then the double integral of the "singular part" is added. Method 3 is preferable to either of methods 1 and 2 because the final numerical integration in methods 1 and 2 may involve a singular integrand. However, if what is deemed to be the "singular part" can be integrated analytically with respect to only one of the variables, then either method 1 or method 2 is applicable, but method 3 is not.

Use of method 1 is now demonstrated. From (56)-(60), the required integrals with respect to t' are

$$G_a = \frac{2}{\Delta_q} \int_{t_q^-}^{t_{q+1}^-} \frac{e^{-jkR_p}}{kR_p} dt' \quad (71)$$

$$G_b = \left(\frac{2}{\Delta_q}\right)^2 \int_{t_q^-}^{t_{q+1}^-} (t' - t_q) \frac{e^{-jkR_p}}{kR_p} dt' \quad (72)$$

The above expressions are rewritten as

$$G_a = G_{a1} + G_{a2} \quad (73)$$

$$G_b = G_{b1} + G_{b2} \quad (74)$$

where

$$G_{a1} = \frac{2}{\Delta_q} \int_{t_q^-}^{t_{q+1}^-} \frac{e^{-jkR_{p-1}}}{kR_p} dt' \quad (75)$$

$$G_{a2} = \frac{2}{\Delta_q} \int_{t_q^-}^{t_{q+1}^-} \frac{dt'}{kR_p} \quad (76)$$

$$G_{b1} = \left(\frac{2}{\Delta_q}\right)^2 \int_{t_q^-}^{t_{q+1}^-} (t' - t_q) \left(\frac{e^{-jkR_{p-1}}}{kR_p}\right) dt' \quad (77)$$

$$G_{b2} = \left(\frac{2}{\Delta_q}\right)^2 \int_{t_q^-}^{t_{q+1}^-} \frac{(t' - t_q) dt'}{kR_p} \quad (78)$$

Application of n_t -point Gaussian quadrature to the right-hand sides of (75) and (77) gives

$$G_{a1} = \sum_{\ell'=1}^{n_t} A_{\ell'}^{(n_t)} G \quad (79)$$

$$G_{b1} = \sum_{\ell'=1}^{n_t} x_{\ell'}^{(n_t)} A_{\ell'}^{(n_t)} G \quad (80)$$

where

$$G = \frac{e^{-jkR_{p-1}}}{kR_p} = \frac{-\sin\left(\frac{kR}{2}\right)\left(\sin\left(\frac{kR}{2}\right) + j \cos\left(\frac{kR}{2}\right)\right)}{\left(\frac{kR}{2}\right)} \quad (81)$$

where R_p is to be evaluated at $(t' - t_q) = \frac{1}{2} \Delta_q x_{\ell'}^{(n_t)}$. The purpose of the alternate form of G on the extreme right-hand side of (81) is to

avoid possible roundoff error. As for the integrals in (76) and (78), we substitute (40) and (61) into (32) to obtain

$$R_p = \sqrt{(\rho_q - \rho_p + (t' - t_q) \sin v_q)^2 + (z_q - z_p + (t' - t_q) \cos v_q)^2} + 4\rho_p (\rho_q + (t' - t_q) \sin v_q) \sin^2 \left(\frac{\phi}{2}\right) \quad (82)$$

which can be rewritten as

$$R_p = \sqrt{(t' - t_q + t_o)^2 + d^2} \quad (83)$$

where

$$t_o = (\rho_q - \rho_p) \sin v_q + (z_q - z_p) \cos v_q + 2\rho_p \sin v_q \sin^2 \left(\frac{\phi}{2}\right) \quad (84)$$

$$d = \sqrt{r_{pq}^2 - t_o^2} \quad (85)$$

$$r_{pq} = \sqrt{(\rho_q - \rho_p)^2 + (z_q - z_p)^2 + 4\rho_q \rho_p \sin^2 \left(\frac{\phi}{2}\right)} \quad (86)$$

Substitution of (83) into (76) and (78) and application of formulas 200.0L and 201.0L of Dwight [6] give

$$G_{a2} = \frac{2}{k\Delta_q} \log \quad (87)$$

$$G_{b2} = \left(\frac{2}{\Delta_q}\right)^2 \frac{1}{k} \left[\sqrt{\left(t_o + \frac{\Delta_q}{2}\right)^2 + d^2} - \sqrt{\left(t_o - \frac{\Delta_q}{2}\right)^2 + d^2} - t_o \log \right] \quad (88)$$

where

$$\log = \left[\frac{\left| t_o \right| + \frac{\Delta q}{2} + \sqrt{\left(\left| t_o \right| + \frac{\Delta q}{2} \right)^2 + d^2}}{\left| t_o \right| - \frac{\Delta q}{2} + \sqrt{\left(\left| t_o \right| - \frac{\Delta q}{2} \right)^2 + d^2}} \right], \quad \left| t_o \right| \geq \frac{\Delta q}{2} \quad (89)$$

$$\log = \left[\frac{\left[\left| t_o \right| + \frac{\Delta q}{2} + \sqrt{\left(\left| t_o \right| + \frac{\Delta q}{2} \right)^2 + d^2} \right] \left[\frac{\Delta q}{2} - \left| t_o \right| + \sqrt{\left(\frac{\Delta q}{2} - \left| t_o \right| \right)^2 + d^2} \right]}{d^2} \right], \quad \left| t_o \right| < \frac{\Delta q}{2}$$

To reduce roundoff error, (88) is rewritten as

$$G_{b2} = \left(\frac{2}{\Delta q} \right) \frac{t_o}{k} \left[\frac{4}{\sqrt{\left(t_o + \frac{\Delta q}{2} \right)^2 + d^2} + \sqrt{\left(t_o - \frac{\Delta q}{2} \right)^2 + d^2}} - \frac{2}{\Delta q} \log \right] \quad (90)$$

The calculated values of G_a are used to obtain G_{ma} according to

$$G_{4a} = \pi \sum_{\ell=1}^{n_\phi} G_a A_\ell^{(n_\phi)} \sin^2 \left(\frac{\phi_\ell}{2} \right) \cos(n\phi_\ell) \quad (91)$$

$$G_{5a} = \frac{\pi}{2} \sum_{\ell=1}^{n_\phi} G_a A_\ell^{(n_\phi)} \cos \phi_\ell \cos(n\phi_\ell) \quad (92)$$

$$G_{6a} = \frac{\pi}{2} \sum_{\ell=1}^{n_\phi} G_a A_\ell^{(n_\phi)} \sin \phi_\ell \sin(n\phi_\ell) \quad (93)$$

where G_a is to be evaluated at $\phi = \phi_\ell$ given by (70). Equations (91)-(93) are also valid with a replaced by b. Calculation of G_a and G_b should be according to the development (73)-(90) only for those values of ϕ_ℓ for which r_{pq} is either smaller than or comparable to Δ_q . If r_{pq} is considerably larger than Δ_q , pure Gaussian quadrature is adequate.

Use of method 2 is now demonstrated. Since the integrands of (58) and (60) are fairly well-behaved, method 2 is applied only to (59).

In method 2, G_{5a} and G_{5b} are calculated according to (62) and (63) with

$G_5(\frac{1}{2} \Delta_q x_{\ell'}^{(n_t)})$ given not by (65) but by

$$G_5(\frac{1}{2} \Delta_q x_{\ell'}^{(n_t)}) = \frac{\pi}{2} \sum_{\ell=1}^{n_\phi} A_\ell^{(n_\phi)} \frac{e^{-jkR_{p\ell'} \ell}}{kR_{p\ell'} \ell} \cos \phi_\ell \cos(n\phi_\ell) -$$

$$- \frac{\pi}{2} \sum_{\ell=1}^{n_\phi} \frac{A_\ell^{(n_\phi)}}{k \sqrt{(\rho' - \rho_p)^2 + (z' - z_p)^2 + \rho' \rho_p \phi^2}}$$

$$+ \int_{\phi=0}^{\pi} \frac{d\phi}{k \sqrt{(\rho' - \rho_p)^2 + (z' - z_p)^2 + \rho' \rho_p \phi^2}} \quad (94)$$

From formula 200.01. of Dwight [6],

$$\int_{\phi=0}^{\pi} \frac{d\phi}{k \sqrt{(\rho' - \rho_p)^2 + (z' - z_p)^2 + \rho' \rho_p \phi^2}} = \frac{1}{k\sqrt{\rho' \rho_p}} \log(u + \sqrt{1+u^2}) \quad (95)$$

where

$$u = \frac{\pi\sqrt{\rho' \rho_p}}{\sqrt{(\rho' - \rho_p)^2 + (z' - z_p)^2}} \quad (96)$$

Equation (94) should be used only for those values of t' for which ρ_q

is considerably larger than $\sqrt{(\rho' - \rho_p)^2 + (z' - z_p)^2}$. Otherwise, the pure Gaussian quadrature of (65) is adequate.

Use of method 3 is now demonstrated for the case in which $p=q$.

Method 3 is applied only to the calculation of G_{5a} because G_{5a} is the only integral in (56) and (57) whose integrand is not bounded. We write

$$G_{5a} = \frac{\pi}{2} \sum_{\ell=1}^{n_\phi} A_\ell^{(n_\phi)} \cos \phi_\ell \cos(n\phi_\ell) \sum_{\ell'=1}^{n_t} A_{\ell'}^{(n_t)} \frac{e^{-jkR_{p\ell'\ell}}}{kR_{p\ell'\ell}} - \quad (97)$$

$$- \frac{\pi}{2} \sum_{\ell=1}^{n_\phi} A_\ell^{(n_\phi)} \sum_{\ell'=1}^{n_t} \frac{A_{\ell'}^{(n_t)}}{k \sqrt{\left(\frac{\Delta_q}{2} x_{\ell'}\right)^2 + \rho_q^2 \phi_\ell^2}} + \frac{2}{\Delta_q} \int_0^\pi d\phi \int_{t_q^-}^{t_q^-+1} \frac{dt'}{k \sqrt{(t'-t_q)^2 + \rho_q^2 \phi^2}}$$

Because of the formula

$$\frac{d^2}{dx dy} [x \log(y + \sqrt{x^2 + y^2}) + y \log(x + \sqrt{x^2 + y^2})] = \frac{1}{\sqrt{x^2 + y^2}}, \quad (98)$$

the double integral in (97) is tractable.

$$\frac{2}{\Delta_q} \int_0^\pi d\phi \int_{t_q^-}^{t_q^-+1} \frac{dt'}{k \sqrt{(t'-t_q)^2 + \rho_q^2 \phi^2}} = \frac{2}{k\rho_q} \left[\log \left[\frac{2\pi\rho_q}{\Delta_q} + \sqrt{1 + \left(\frac{2\pi\rho_q}{\Delta_q}\right)^2} \right] + \right. \\ \left. + \frac{2\pi\rho_q}{\Delta_q} \log \left[\frac{\Delta_q}{2\pi\rho_q} + \sqrt{1 + \left(\frac{\Delta_q}{2\pi\rho_q}\right)^2} \right] \right] \quad (99)$$

In each of methods 1, 2, and 3, an attempt is made to subtract out the singularity due to $1/R_p$ in (58)-(60). In method 1, $1/R_p$ itself is subtracted out. In method 2, the approximation

$$\frac{1}{\sqrt{(\rho' - \rho_p)^2 + (z' - z_p)^2 + \rho_p \rho' \phi^2}}$$

to $1/R_p$ is subtracted out. For comparison, R_p is given by (32). In method 3, the approximation

$$\frac{1}{\sqrt{(\rho' - \rho_p)^2 + (z' - z_p)^2 + \rho_p \rho_q \phi^2}}$$

to $1/R_p$ is subtracted out for $p=q$. Because the double integral of this approximation is tractable, method 3 can be extended to cover the case in which $p \neq q$. For $p \neq q$, the alternate approximation

$$\frac{1}{\sqrt{(\rho' - \rho_p)^2 + (z' - z_p)^2 + \rho_p \rho_{\min} \phi^2}}$$

to $1/R_p$ merits consideration. Here, ρ_{\min} is the value of ρ' at that value of t' which minimizes $(\rho' - \rho_p)^2 + (z' - z_p)^2$. No matter which of the above two approximations to $1/R_p$ is used, the closed form expression for its double integral is rather complicated and vulnerable to roundoff error. For this reason, method 3 was used only for $p=q$.

For $p \neq q$, the decision whether to use methods 1 or 2 is based on comparisons of Δ_q with d_o and ρ_q with d_o where d_o is the distance from the field point at $t = t_p$ to the nearest point on the q th source segment. The distance between the field point at $t = t_p$ and the point (t', ϕ) on the q th source segment is given by (82) or (83). It is evident that the minimum of (82) occurs at $\phi = 0$ because neither ρ_p nor ρ' of (40) can be negative. At $\phi = 0$, (84) and (85) specialize to

$$t_o^* = (\rho_q - \rho_p) \sin v_q + (z_q - z_p) \cos v_q \quad (100)$$

$$d^* = |(\rho_q - \rho_p) \cos v_q - (z_q - z_p) \sin v_q| \quad (101)$$

The asterisk (*) on the left-hand sides of (100) and (101) indicates that $\phi = 0$. Minimizing (83) with respect to t' on the q th source segment where $-\frac{\Delta_q}{2} \leq t' - t_q \leq \frac{\Delta_q}{2}$, we obtain

$$d_o = \begin{cases} d^* & |t_o^*| \leq \frac{\Delta q}{2} \\ \sqrt{(|t_o^*| - \frac{\Delta q}{2})^2 + (d^*)^2} & |t_o^*| > \frac{\Delta q}{2} \end{cases} \quad (102)$$

If

$$\left. \begin{array}{l} p \neq q \\ \frac{1}{2} c_t \Delta q \leq d_o \\ c_\phi \rho_q \leq d_o \end{array} \right\} \begin{array}{l} \text{Case 1} \\ \text{Pure quadrature} \end{array} \quad (103)$$

then the pure quadrature of (62) - (66) is used to calculate G_{ma} and G_{mb} . Here, c_t and c_ϕ are constants for which the values

$$\begin{aligned} c_t &= 2. \\ c_\phi &= 0.1 \end{aligned} \quad (104)$$

are suggested. If

$$\left. \begin{array}{l} p \neq q \\ \frac{1}{2} c_t \Delta q > d_o \\ c_\phi \rho_q \leq d_o \end{array} \right\} \begin{array}{l} \text{Case 2} \\ \text{Method 1} \end{array} \quad (105)$$

then method 1 is used. If

$$\left. \begin{array}{l} p \neq q \\ c_\phi \rho_q > d_o \end{array} \right\} \begin{array}{l} \text{Case 3} \\ \text{Method 2} \end{array} \quad (106)$$

then method 2 is used. If

$$\left. \begin{array}{l} p = q \end{array} \right\} \begin{array}{l} \text{Case 4} \\ \text{Methods 1 and 3} \end{array} \quad (107)$$

then both methods 1 and 3 are used.

31

The strategy in (103) and (105)-(107) is based on the assumptions that the Gaussian quadrature integration with respect to t' must be fortified only when Δ_q is large, and that the Gaussian quadrature integration with respect to ϕ must be fortified only when ρ_q is large. The integration with respect to t' could not be fortified for $\frac{1}{2} c_t \Delta_q > d_o$ in Case 3 because methods 1 and 2 can not be applied simultaneously and because it was decided earlier to limit use of method 3 to Case 4. However, pure Gaussian quadrature should still give a fairly accurate evaluation of this integral with respect to t' because of the following reasoning. Since ρ' is large, difficulty can only occur when ϕ is small. Furthermore, this difficulty is not usually serious because $\Delta_q \leq 2d_o$ most often. It is evident that $\Delta_q \leq 2d_o$ if $p \neq q$, if all the Δ_q are equal, and if the generating curve does not fold back on itself.

IV. EVALUATION OF THE PLANE WAVE EXCITATION VECTOR

Consider the elements (7) and (8) of the excitation vector for a θ -polarized incident plane wave defined by

$$\underline{E}^i = u_{\theta}^t k \eta \underline{e}^{-jk_t \cdot \underline{r}} \quad (108)$$

and also for a ϕ -polarized incident plane wave defined by

$$\underline{E}^i = u_{\phi}^t k \eta \underline{e}^{-jk_t \cdot \underline{r}} \quad (109)$$

In (108) and (109),

$$\underline{k}_t = -k(\underline{u}_x \sin \theta_t + \underline{u}_z \cos \theta_t) \quad (110)$$

$$\underline{u}_{\theta}^t = \underline{u}_x \cos \theta_t - \underline{u}_z \sin \theta_t \quad (111)$$

$$\underline{u}_{\phi}^t = \underline{u}_y \quad (112)$$

where θ_t is the angle of incidence and where \underline{u}_x , \underline{u}_y , and \underline{u}_z are unit vectors in the x, y, and z directions, respectively. Also, \underline{r} is the radius vector from the origin. The origin must lie on the axis of the body of revolution because this axis is the z axis. Substitution of (4), (5), and (108) into (7) and (8) gives

$$V_{ni}^{t\theta} = j^n \pi k \int_{t_i^-}^{t_i^{+2}} dt T_i(t) \{ j \sin v \cos \theta_t (J_{n+1} - J_{n-1}) - 2 \cos v \sin \theta_t J_n \} e^{jkz \cos \theta_t} \quad (113)$$

$$V_{ni}^{\phi\theta} = j^n \pi k \int_{t_i^-}^{t_i^{+1}} dt \frac{\rho}{\rho_i} P_i(t) (J_{n+1} + J_{n-1}) \cos \theta_t e^{jkz \cos \theta_t} \quad (114)$$

where $V_{ni}^{t\theta}$ is V_{ni}^t for \underline{E}^i given by (108) and $V_{ni}^{\phi\theta}$ is V_{ni}^{ϕ} for \underline{E}^i given by (109). In (113) and (114),

$$J_n = J_n(k\rho \sin \theta_t) \quad (115)$$

where J_n is the Bessel function of the first kind. Likewise, substitution of (4), (5), and (109) into (7) and (8) gives

$$V_{ni}^{t\phi} = -j^n \pi k \int_{t_i^-}^{t_{i+2}^-} dt T_i(t) (J_{n+1} + J_{n-1}) \sin v e^{jkz \cos \theta_t} \quad (116)$$

$$V_{ni}^{\phi\phi} = j^{n+1} \pi k \int_{t_i^-}^{t_{i+1}^-} dt \frac{\rho}{\rho_i} P_i(t) (J_{n+1} - J_{n-1}) e^{jkz \cos \theta_t} \quad (117)$$

where the second superscript on V on the left-hand sides of (116) and (117) denotes excitation by the ϕ -polarized incident plane wave (109). The manipulations required to obtain (113)-(117) are similar to those used in the derivation of (1-95).

The contributions to (113) and (116) due to integration with respect to t from t_p^- to t_{p+1}^- are expressed by

$$V_{ni}^{*t\theta} = j^n \pi k \int_{t_p^-}^{t_{p+1}^-} dt T_i(t) \{j \sin v \cos \theta_t (J_{n+1} - J_{n-1}) - 2 \cos v \sin \theta_t J_n\} e^{jkz \cos \theta_t} \quad (118)$$

$$V_{ni}^{*t\phi} = -j^n \pi k \int_{t_p^-}^{t_{p+1}^-} dt T_i(t) (J_{n+1} + J_{n-1}) \sin v e^{jkz \cos \theta_t} \quad (119)$$

where i is either $p-1$ or p . The asterisk (*) on the left-hand sides of (118) and (119) denotes the contribution due to integration from t_p^- to t_{p+1}^- . First, v is replaced by v_p in (118) and (119). Throughout (114), (117), (118), and (119), $P_i(t)$, $T_i(t)$, and ρ are expressed according to

(36), (37), and (40), respectively. Then, i is replaced by p in (114) and (117) to make those equations compatible with (118) and (119). The results of the above substitutions are

$$V_{ni}^{*t\theta} = \frac{j^n \pi k}{2} \int_{t_p}^{t_{p+1}} dt \left(1 + \frac{(-1)^{p-1} 2(t-t_p)}{\Delta_p} \right) \{ j \sin v_p \cos \theta_t (J_{n+1} - J_{n-1}) - 2 \cos v_p \sin \theta_t J_n \} e^{jkz \cos \theta_t} \quad (120)$$

$$V_{np}^{\phi\theta} = j^n \pi k \int_{t_p}^{t_{p+1}} dt \left(1 + \frac{(t-t_p) \sin v_p}{\rho_p} \right) (J_{n+1} + J_{n-1}) \cos \theta_t e^{jkz \cos \theta_t} \quad (121)$$

$$V_{ni}^{*t\phi} = -\frac{j^n \pi k}{2} \int_{t_p}^{t_{p+1}} dt \left(1 + \frac{(-1)^{p-1} 2(t-t_p)}{\Delta_p} \right) (J_{n+1} + J_{n-1}) \sin v_p e^{jkz \cos \theta_t} \quad (122)$$

$$V_{np}^{\phi\phi} = j^{n+1} \pi k \int_{t_p}^{t_{p+1}} dt \left(1 + \frac{(t-t_p) \sin v_p}{\rho_p} \right) (J_{n+1} - J_{n-1}) e^{jkz \cos \theta_t} \quad (123)$$

where i is either $p-1$ or p in (120) and (122).

Equations (120)-(123) can be rewritten as

$$V_{ni}^{*t\theta} = \frac{j^{n+1} \pi k \Delta_p \sin v_p \cos \theta_t}{4} (F_{n+1,a} - F_{n-1,a}) - \frac{j^n \pi k \Delta_p \cos v_p \sin \theta_t}{2} F_{na} + (-1)^{p-1} \left\{ \frac{j^{n+1} \pi k \Delta_p \sin v_p \cos \theta_t}{4} (F_{n+1,b} - F_{n-1,b}) - \frac{j^n \pi k \Delta_p \cos v_p \sin \theta_t}{2} F_{nb} \right\} \quad (124)$$

$$V_{np}^{\phi\theta} = \frac{j^n \pi k \Delta_p \cos \theta_t}{2} \left\{ (F_{n+1,a} + F_{n-1,a}) + \frac{\Delta_p \sin v_p}{2 \rho_p} (F_{n+1,b} + F_{n-1,b}) \right\} \quad (125)$$

$$V_{ni}^{\phi} = -\frac{j^n \pi k \Delta \sin v_p}{4} (F_{n+1,a} + F_{n-1,a}) - \frac{(-1)^{p-i} j^n \pi k \Delta \sin v_p}{4} (F_{n+1,b} + F_{n-1,b}) \quad (126)$$

$$V_{np}^{\phi\phi} = \frac{j^{n+1} \pi k \Delta}{2} \left\{ (F_{n+1,a} - F_{n-1,a}) + \frac{\Delta \sin v_p}{2\rho_p} (F_{n+1,b} - F_{n-1,b}) \right\} \quad (127)$$

where i is either $p-1$ or p in (124) and (126). In (124)-(127),

$$F_{ma} = \frac{2}{\Delta_p} \int_{t_p}^{t_{p+1}} J_m(k\rho \sin \theta_t) e^{jkz \cos \theta_t} dt \quad (128)$$

$m=n-1, n, n+1$

$$F_{mb} = \left(\frac{2}{\Delta_p}\right)^2 \int_{t_p}^{t_{p+1}} (t-t_p) J_m(k\rho \sin \theta_t) e^{jkz \cos \theta_t} dt \quad (129)$$

where, from (40) and (61),

$$\rho = \rho_p + (t-t_p) \sin v_p \quad (130)$$

$$z = z_p + (t-t_p) \cos v_p \quad (131)$$

Evaluation of (128) and (129) by means of an n_T -point Gaussian quadrature formula yields

$$F_{ma} = \sum_{\ell=1}^{n_T} A_{\ell}^{(n_T)} J_m(k\delta_{\ell} \sin \theta_t) e^{jk\hat{z}_{\ell} \cos \theta_t} \quad (132)$$

$m=n-1, n, n+1$

$$F_{mb} = \sum_{\ell=1}^{n_T} A_{\ell}^{(n_T)} x_{\ell}^{(n_T)} J_m(k\delta_{\ell} \sin \theta_t) e^{jk\hat{z}_{\ell} \cos \theta_t} \quad (133)$$

where

$$\hat{\rho}_\ell = \rho_p + \frac{\Delta_p x_\ell^{(n_T)}}{2} \sin v_p \quad (134)$$

$$\hat{z}_\ell = z_p + \frac{\Delta_p x_\ell^{(n_T)}}{2} \cos v_p \quad (135)$$

The calculation of the plane wave excitation vector would be most nearly consistent with the calculation of the moment matrix if $n_T = 1$. For $n_T = 1$, the extra data $x_1^{(1)} = 0$ and $A_1^{(1)} = 2$ must be supplied. Now, assuming that $n_t > 1$, it could be said that n_t -point quadrature is more accurate than 1-point quadrature. The n_t -point quadrature data are already available because they were used to calculate the elements of the moment matrix in Section III. With n_t fixed at 2, results were calculated for both $n_T = 1$ and $n_T = 2$. It was difficult to tell which results were more accurate. The numerical results presented in Section V were obtained by using $n_t = n_T = 2$.

V. NUMERICAL RESULTS

Computer program subroutines have been written to calculate the elements of the moment matrix and the elements of the plane wave excitation vector. These subroutines are described and listed in Part Two of this report. They were used to calculate the electric currents induced by a plane wave axially incident on two circular disks, a thin washer, a cone-sphere, an open cylinder, and a spherical shell with an axially symmetric aperture. The magnitudes of these electric currents are plotted in this section.

For axial incidence, θ_t is either 0° or 180° and the only non-zero excitation vectors for the θ -polarized plane wave (108) are

$$\begin{bmatrix} \vec{V}_{-1}^t \\ \vec{V}_{-1}^\phi \end{bmatrix} = \begin{bmatrix} \vec{V}_1^t \\ -\vec{V}_1^\phi \end{bmatrix} \quad (136)$$

It is evident from (9)-(17) that

$$\begin{bmatrix} Z_{-1}^{tt} & Z_{-1}^{t\phi} \\ Z_{-1}^{\phi t} & Z_{-1}^{\phi\phi} \end{bmatrix} = \begin{bmatrix} Z_1^{tt} & -Z_1^{t\phi} \\ -Z_1^{\phi t} & Z_1^{\phi\phi} \end{bmatrix} \quad (137)$$

In consequence of (136), (137), and (6), the only non-zero column vectors \vec{I}_n^t and \vec{I}_n^ϕ are given by

$$\begin{bmatrix} \vec{I}_{-1}^t \\ \vec{I}_{-1}^\phi \end{bmatrix} = \begin{bmatrix} \vec{I}_1^t \\ -\vec{I}_1^\phi \end{bmatrix} \quad (138)$$

where the column vector on the right-hand side of (138) satisfies (6) for $n=1$.

In view of (2) and (3), substitution of (138) into (1) and subsequent division by k give

$$\frac{\underline{J}}{|\underline{H}^i|} = 2\underline{u}_t \cos \phi \left(\sum_j I_{1j}^t \frac{T_j(t)}{k\rho} \right) + 2j \underline{u}_\phi \sin \phi \left(\sum_j I_{1j}^\phi \frac{P_j(t)}{k\rho_j} \right) \quad (139)$$

The $|\underline{H}^i|$ written instead of k on the left-hand side of (139) is the magnitude of the incident magnetic field associated with (108). This $|\underline{H}^i|$ is indeed equal to k . At $t = t_{p+1}^-$, the t component of (139) reduces to

$$\frac{J_t}{|\underline{H}^i|} = \frac{2I_{1p}^t}{k\rho(t_{p+1}^-)} \cos \phi, \quad p=1,2,\dots,P-2 \quad (140)$$

At $t = t_p$, the ϕ component of (139) reduces to

$$\frac{J_\phi}{|\underline{H}^i|} = \frac{2jI_{1p}^\phi}{k\rho_p} \sin \phi, \quad p=1,2,\dots,P-1 \quad (141)$$

Here, J_t and J_ϕ are, respectively, the t and ϕ components of \underline{J} . In the figures to follow, $\frac{|J_t|}{|\underline{H}^i|}$ in the $\phi = 0^\circ$ plane is plotted with squares and $\frac{|J_\phi|}{|\underline{H}^i|}$ in the $\phi = 90^\circ$ plane is plotted with octagons.

Figure 4 shows the t and ϕ components $\frac{|J_t|}{|\underline{H}^i|}$ and $\frac{|J_\phi|}{|\underline{H}^i|}$ of the electric current induced by the axially incident electric field (108) with $\theta_t = 0$ on an infinitely thin circular disk of radius 0.25λ where λ is the wavelength. In Fig. 4, $\frac{|J_t|}{|\underline{H}^i|}$ is plotted with squares and $\frac{|J_\phi|}{|\underline{H}^i|}$ with octagons.

Both quantities are plotted versus t/λ where t is the arc length along the generating curve. The horizontal axis in Fig. 4 was labeled T/λ because the lower case letter t could not be drawn by the plotter. In Fig. 4, the center of the disk is at $t = 0$ and the edge at $t = 0.25\lambda$. The electric currents in Fig. 4 and in Figs. 5-10 to follow were calculated with $n_t = n_T = 2$, $n_\phi = 20$ and with the points t_j^- , $j=1,2,\dots,P$ equally spaced along the generating curve. Since 12 octagons are in Fig. 4, $P=13$ therein. The electric current in Fig. 4 should be twice as large as the magnetic current in Fig. 4 on page 32 of [7].

Figure 5 shows the electric current induced on a circular disk of radius 1.5λ by the same axially incident plane wave as in Fig. 4. The electric current in Fig. 5 should be twice as large as the magnetic current in Fig. 6 on page 33 of [7]. Figure 6 shows the electric current for axial incidence on an infinitely thin washer of inner radius 0.4λ and outer radius 1.2λ . The inner edge of the washer is at $t = 0$ and the outer edge at $t = 0.8\lambda$. Figure 6 should be compared with Fig. 3 of [8]. The size of the washer in Fig. 3 of [8] is incorrectly stated. That figure is actually a plot of the electric current on the same washer as in Fig. 6.

Figures 7 and 8 are plots of the electric current for axial incidence on a cone-sphere of cone angle 20° and sphere radius 0.2λ . Figure 7 is for incidence on the sphere end and Fig. 8 is for incidence on the tip of the cone. The tip of the cone is at $t = 0$. At the sphere end, t is approximately 1.48λ . For comparison, see Fig. 4.15 on page 218 of [9].

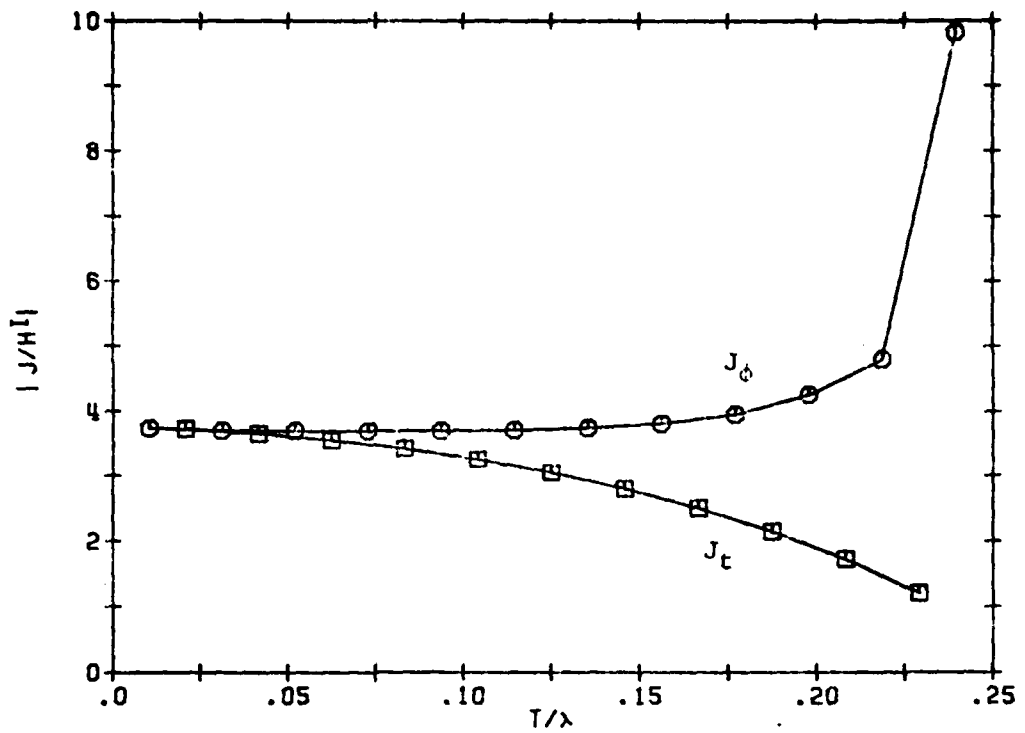


Fig. 4. Electric current for axial incidence on a circular disk of radius 0.25λ , $\tau = 0$ at center.

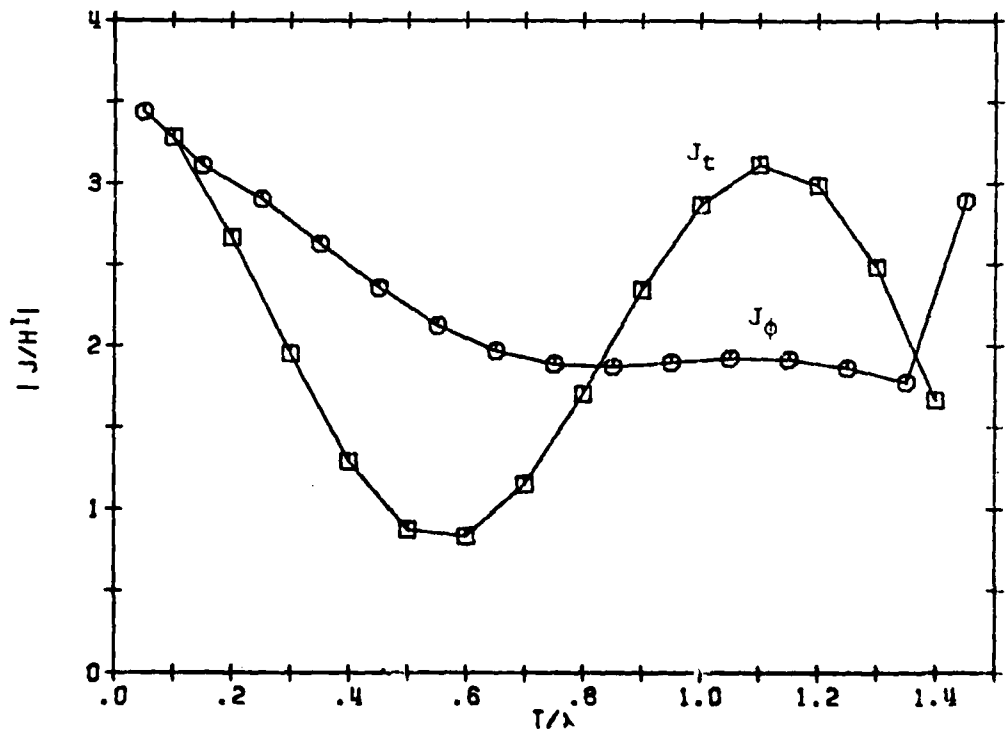


Fig. 5. Electric current for axial incidence on a circular disk of radius 1.5λ , $\tau = 0$ at center.

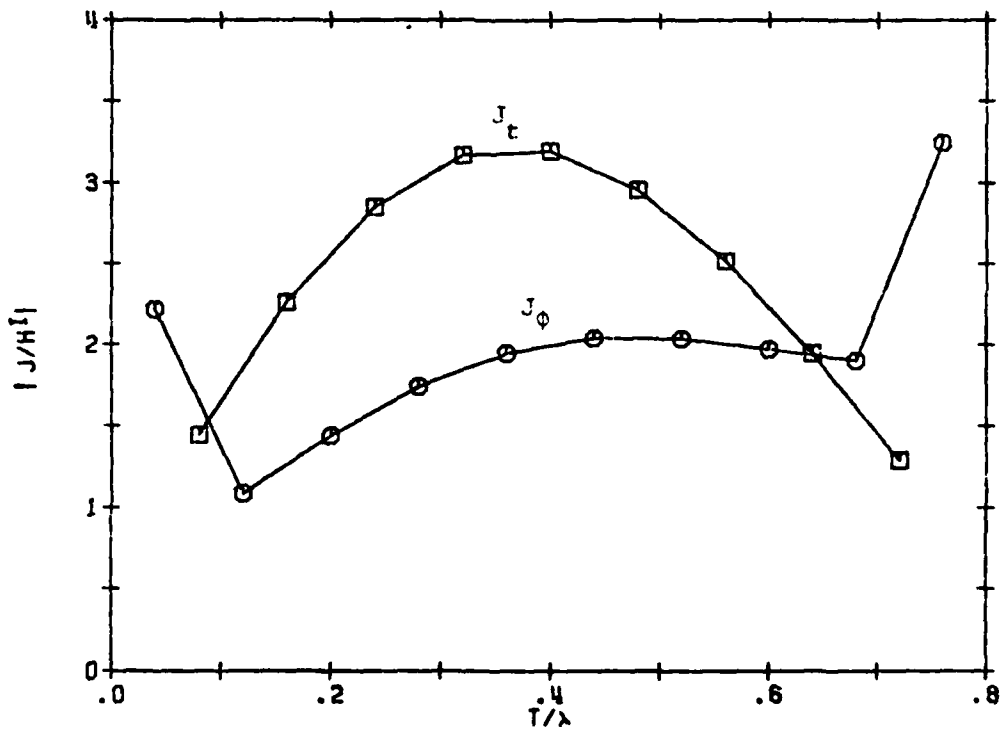


Fig. 6. Electric current for axial incidence on a circular washer of inside radius 0.4λ and outside radius 1.2λ , $t = 0$ at inside edge.

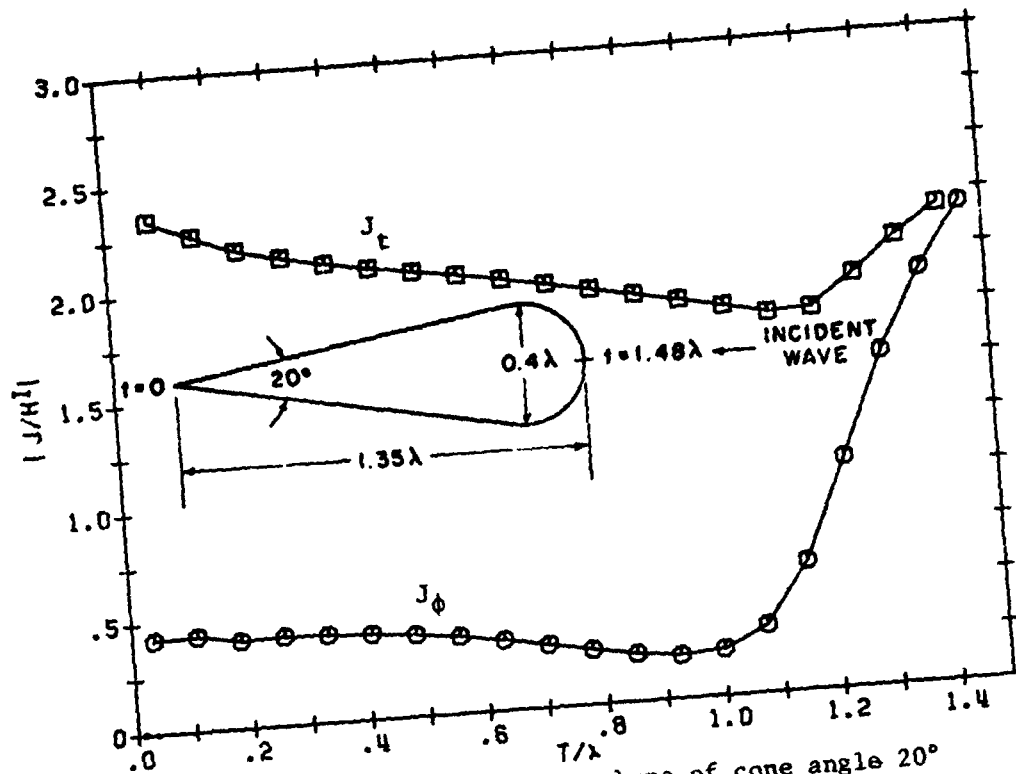


Fig. 7. Electric current on a cone-sphere of cone angle 20° and sphere radius 0.2λ , incidence on sphere.

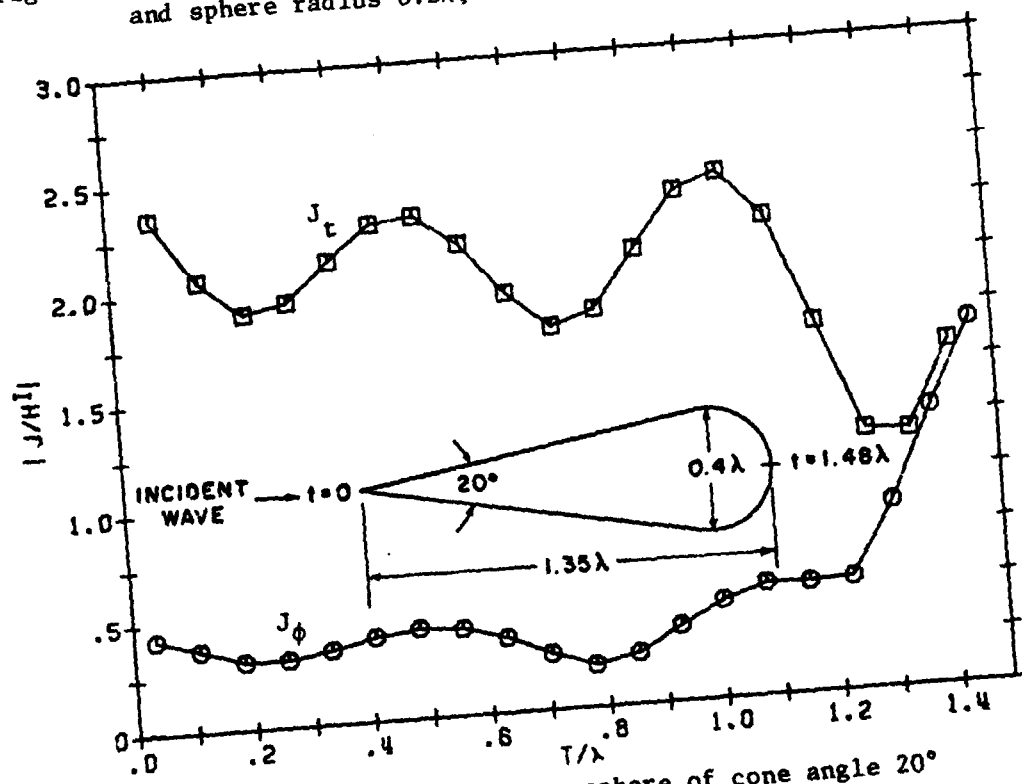


Fig. 8. Electric current on a cone-sphere of cone angle 20° and sphere radius 0.2λ , incidence on tip.

Figure 9 shows the electric current for axial incidence on an open-ended cylinder of radius $\lambda/2\pi$ and length λ . The plane wave is incident on the end of the cylinder for which $t = 0$. The excellent results plotted in Fig. 9 here and in Fig. 2.13 on page 52 of [2] were both obtained by using the electric field integral equation, notwithstanding the stability problem reported in [10].

Figure 10 is a plot of the electric current for axial incidence on the infinitely thin conducting shell for which

$$r = 0.2\lambda$$
$$45^\circ \leq \theta \leq 180^\circ$$

where r and θ , being spherical coordinates, are the radius and colatitude, respectively. This shell is a spherical shell with an axially symmetric aperture. The pole of the shell is at $t = 0$. At the edge of the shell, t is approximately 0.471λ . The plane wave is incident on the aperture.

Numerical results for the electric current on a circular disk of radius 0.02λ not shown here exhibited a noticeable change in slope near the center of the disk. The curves labeled "a" in Figs. 7 and 8 on page 34 of [7] also indicate a change in the slope of the magnetic current near the center of the complementary aperture. However, these changes in slope did not agree with each other. Now, equation (23) of [11] does not predict any noticeable change in the slope of the electric current near the center of the disk of radius 0.02λ . The changes in slope obtained by using the computer program of the present

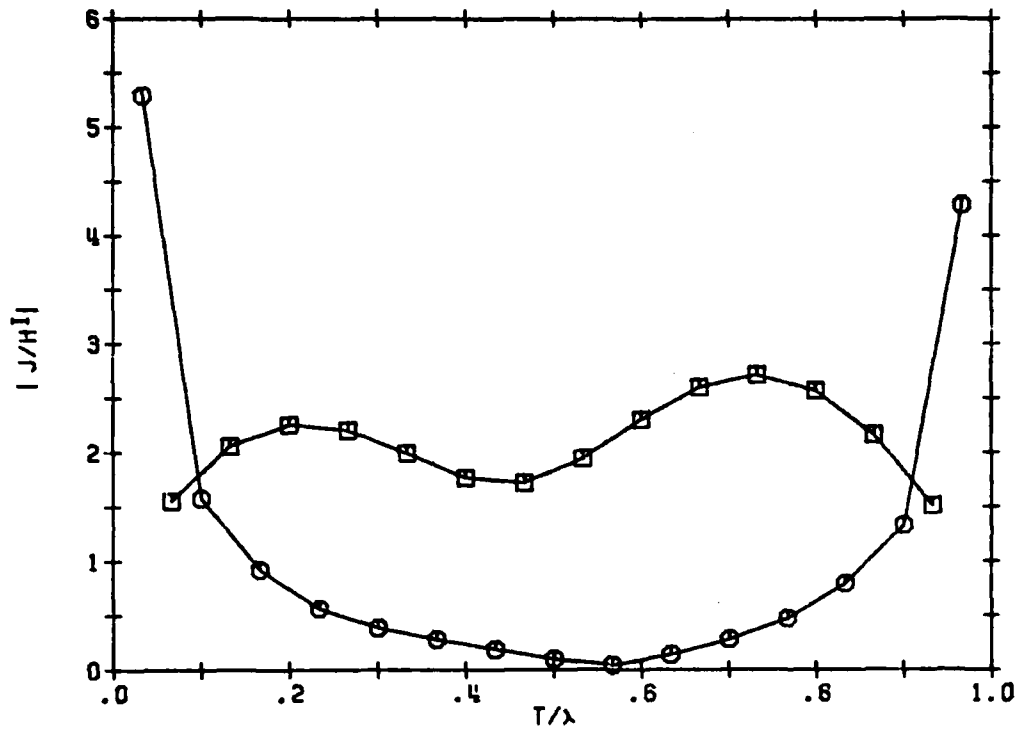


Fig. 9. Electric current on an open-ended cylinder of radius $\lambda/(2\pi)$ and length λ , incidence on $t = 0$.

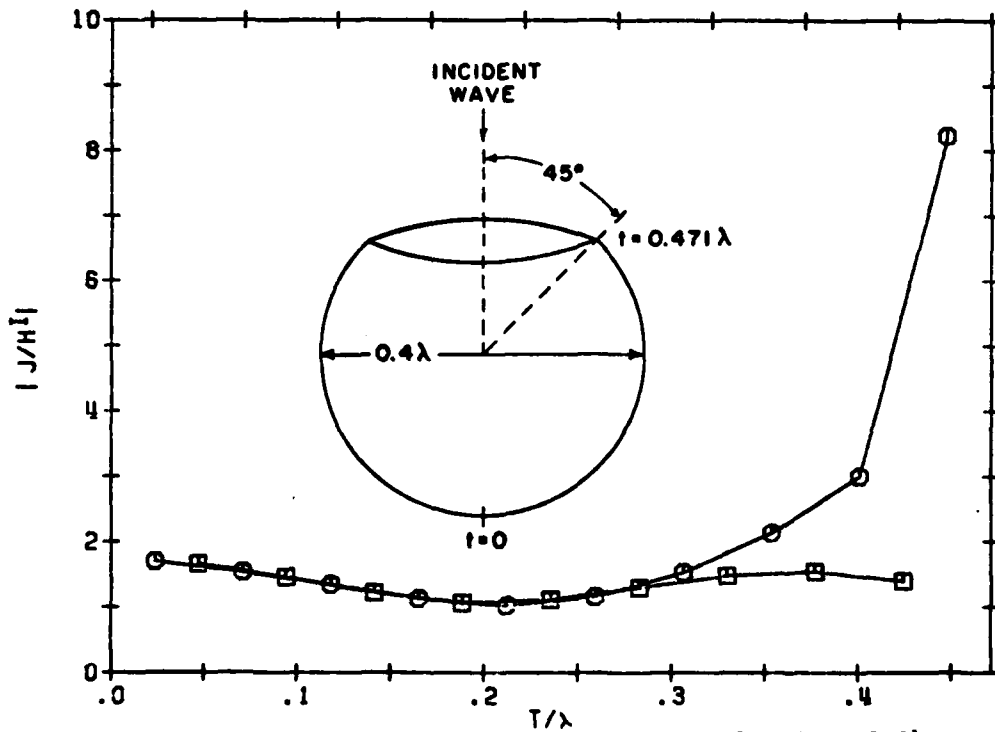


Fig. 10. Electric current on a spherical shell of radius 0.2λ with axially symmetric aperture, edge at $t = 0.471\lambda$, incidence on aperture.

report and the program of [7] are obviously wrong. The changes in slope obtained by using these programs are much more pronounced for the disk of radius 0.002λ . However, they disappear when all calculations are done in double precision. Hence, these changes in slope are due to severe roundoff error. This roundoff error occurs because the vector potential terms, those containing the factor k^2 explicit in (9)-(12), are overshadowed by the rest of the terms in (9)-(12), the scalar potential terms. If these vector potential terms were set equal to zero, the moment matrix would be singular because there are several linear combinations of the expansion functions which have no electric charge associated with them.

PART TWO
COMPUTER PROGRAM

I. INTRODUCTION

The computer program which implements the numerical solution expounded in Part One is described and listed here in Part Two. This program consists of the subroutine ZMAT, the function BLOG, the subroutines PLANE, DECOMP, and SOLVE, and a main program. The subroutine ZMAT calculates the elements of the moment matrix in (6). The function BLOG is called by ZMAT. The subroutine PLANE calculates the elements of the excitation vector in (6) for plane wave incidence. The subroutines DECOMP and SOLVE solve the matrix equation (6) for \vec{I}_n^t and \vec{I}_n^ϕ .

The main program obtains the electric current induced on the surface of the body of revolution by the axially incident plane wave (108) with $\theta_t = 0$ or π radians. The main program calls the subroutines ZMAT, PLANE, DECOMP, and SOLVE. It is not difficult to generalize the main program to oblique incidence because the subroutines ZMAT, PLANE, DECOMP, and SOLVE are designed to calculate \vec{I}_n^t and \vec{I}_n^ϕ for $n = 0, 1, 2, \dots$. For the θ -polarized incident plane wave (108), \vec{I}_n^t is even in n and \vec{I}_n^ϕ is odd in n . For the ϕ polarization (109), \vec{I}_n^t is odd in n and \vec{I}_n^ϕ is even in n . In order to obtain far field patterns, the main program must be supplied with additional logic. This additional logic is outlined as follows. According to (1-91), the far field is obtained by premultiplying the solution vector to (6) by plane wave measurement matrices for $n = 0, \pm 1, \pm 2, \dots$. The plane wave measurement matrices for $n = 0, 1, 2, \dots$

can be obtained by calling the subroutine PLANE. The even-odd behavior in n of the coefficient of $e^{jn\phi_r}$ in (1-91) is as follows.

Receiver Polarization	Transmitter Polarization	Behavior in n
θ	θ	even in n
ϕ	θ	odd in n
θ	ϕ	odd in n
ϕ	ϕ	even in n

Here, the receiver polarization denotes the component of the far field being measured. The transmitter polarization is the polarization of the incident plane wave.

II. THE SUBROUTINE ZMAT

The subroutine ZMAT(M1,M2,NP,NPHI,NT,RH,ZH,X,A,XT,AT,Z) calculates the moment matrices in (6) for $n = M1, M1+1, \dots, M2$ where $M1 \geq 0$ and stores them in Z. Z is the only output argument. The rest of the arguments of ZMAT are input arguments. For $n = M1$, storage of the Z_n submatrices in Z is as follows.

$$(Z_n^{tt})_{ij} \text{ in } Z(i+N*(j-1))$$

$$(Z_n^{\phi t})_{ij} \text{ in } Z(i+N*(j-1) + NP-2)$$

$$(Z_n^{t\phi})_{ij} \text{ in } Z(i+N*(j-1) + (NP-2)*N)$$

$$(Z_n^{\phi\phi})_{ij} \text{ in } Z(i+N*(j-1) + (NP-2)*N+NP-2)$$

Here,

$$N = 2*NP-3 \quad (142)$$

For $n > M1$, the Z_n submatrices are stored in $Z((n-M1)*N*N+1)$ to $Z((n-M1+1)*N*N)$ in the same manner as the Z_n submatrices were stored in $Z(1)$ to $Z(N*N)$ for $n = M1$. Table 1 relates the third to eleventh arguments of ZMAT to variables in Part One of the text. In Table 1, $\rho(t_i^-)$ and $z(t_i^-)$ are the values of ρ and z at $t = t_i^-$ for $i = 1, 2, \dots, P$.

Table 1. Third to eleventh arguments of ZMAT.

Argument of ZMAT	Variables in Part One
NP	P
NPHI	n_ϕ
NT	n_t
RH	$k\rho(t_1^-), k\rho(t_2^-), \dots, k\rho(t_p^-)$
ZH	$kz(t_1^-), kz(t_2^-), \dots, kz(t_p^-)$
X	$x_1^{(n_\phi)}, x_2^{(n_\phi)}, \dots, x_{n_\phi}^{(n_\phi)}$
A	$A_1^{(n_\phi)}, A_2^{(n_\phi)}, \dots, A_{n_\phi}^{(n_\phi)}$
XT	$x_1^{(n_t)}, x_2^{(n_t)}, \dots, x_{n_t}^{(n_t)}$
AT	$A_1^{(n_t)}, A_2^{(n_t)}, \dots, A_{n_t}^{(n_t)}$

Minimum allocations are given by

COMPLEX Z(M3*N*N), G4A(M3), G5A(M3), G6A(M3),
 G4B(M3), G5B(M3), G6B(M3), GA(NPHI), GB(NPHI)
 DIMENSION RH(NP), ZH(NP), X(NPHI), A(NPHI),
 XT(NT), AT(NT), RS(NP-1), ZS(NP-1), D(NP-i),
 DR(NP-1), DZ(NP-1), DM(NP-1), C2(NPHI),
 C3(NPHI), R2(NT), Z2(NT), C4(M3*NPHI), C5(M3*NPHI),
 C6(M3*NPHI), Z7(NT), R7(NT), Z8(NT), R8(NT)

where $M3 = M2 - M1 + 1$.

The elements of the Z_n submatrices are calculated according to (48)-(51) where G_{ma} and G_{mb} are given by (54), (55), and (62)-(66). However, (62)-(66) are modified through the use of methods 1, 2, or 3 in the cases specified by (105)-(107). The values of c_t and c_ϕ suggested in (104) enter via CT and CP in lines 10 and 11.

DO loop 10 sets

$$\begin{aligned} RS(q) &= k\rho_q & DR(q) &= \frac{k\Delta}{2} \sin v_q \\ ZS(q) &= kz_q & DZ(q) &= \frac{k\Delta}{2} \cos v_q \\ D(q) &= \frac{k\Delta}{2} & DM(q) &= \frac{\Delta}{2\rho_q} \end{aligned}$$

for $q = 1, 2, \dots, NP-1$.

DO loop 11 sets

$$C2(K) = \phi_K^2 \quad \text{and} \quad C3(K) = 4 \sin^2\left(\frac{\phi_K}{2}\right).$$

Inner DO loop 29 sets

$$\begin{aligned} C4(M5) &= \pi A_K^{(n,\phi)} \sin^2\left(\frac{\phi_K}{2}\right) \cos(n\phi_K) \\ C5(M5) &= \frac{\pi}{2} A_K^{(n,\phi)} \cos \phi_K \cos(n\phi_K) \\ C6(M5) &= \frac{\pi}{2} A_K^{(n,\phi)} \sin \phi_K \sin(n\phi_K) \end{aligned}$$

where $M5 = K + (n-1)*NPHI$.

The calculation of (48)-(51) occurs inside three DO loops nested in the following manner.

DO 15 JQ = 1, MP

DO 16 IP = 1, MP

DO 31 M = 1, M3

CALCULATION OF (48)-(51)

31 CONTINUE
 16 CONTINUE
 15 CONTINUE

Here, JQ, IP, and M represent, respectively, the variables q, p, and (n-Ml+1) in (48)-(51). The JN introduced in line 52 is incremented in line 314 so that the subscript for $(z_n^{tt})_{p-1,q-1}$ can be written as p + JN when n = Ml. The variable KQ defined in lines 54 to 56 keeps track of the cases for which q = 1 and q = MP. Because of (24), these cases require special treatment. According to (24), expressions (48) and (49) are absent when j = q-1 and q = 1. Likewise, (48) and (49) are absent when j = q and q = MP.

The variables defined in statements 57 to 70 are needed inside DO loop 12 or DO loop 16. DO loop 12 puts $k\rho'$ and kz' of (68) and (69) in R2 and Z2, respectively. To reduce execution time, references to subscripted variables as well as calculations are being done outside DO loops whenever possible. Unfortunately, this usually increases the number of statements and complicates the logic because factors such as $\frac{jk^2 \Delta \Delta}{8 p q} \sin v_p \sin v_q$ in (48) are computed by means of several statements scattered throughout the program. One way to follow the gradual building up of constants from outer to inner DO loops is to tabulate computer program variables versus variables in Part One of the text.

Lines 78 to 88 put kd_0 of (102) in D6. Lines 89 to 94 set KP equal to the case number in (103) and (105)-(107).

Lines 96 to 248 put approximate values of G_{ma} of (56) in GmA for $m = 4,5,6$. Lines 96 to 248 also put approximate values of G_{mb} of (57) in GmB for $m = 4,5,6$.

Lines 96 to 174 are executed for case 2 of (105) and for case 4 of (107). Method 1 is used here. This method is described by (71)-(93). The pure Gaussian quadrature option for G_a and G_b advocated just after (93) is

$$G_a = \sum_{\ell'=1}^{n_t} A_{\ell'}^{(n_t)} \frac{e^{-jkR_p}}{kR_p} \quad (143)$$

$$G_b = \sum_{\ell'=1}^{n_t} A_{\ell'}^{(n_t)} x_{\ell'}^{(n_t)} \frac{e^{-jkR_p}}{kR_p} \quad (144)$$

where R_p has the same meaning as in (81). In terms of Z7, R7, Z8, and R8 calculated by DO loop 40,

$$kR_p = \sqrt{Z7(\ell') + R7(\ell')*(4 \sin^2(\frac{\phi}{2}))} \quad (145)$$

$$\frac{kR_p}{2} = \sqrt{Z8(\ell') + R8(\ell')*(4 \sin^2(\frac{\phi}{2}))} \quad (146)$$

DO loop 33 puts G_a and G_b in GA(K) and GB(K). The index K of DO loop 33 corresponds to ℓ in (91)-(93). Line 109 puts $k^2 r_{pq}^2$ of (86) in RR. If

$$r_{pq} < \frac{1}{2} c_t \Delta_q + \frac{1}{2} \Delta_q \quad (147)$$

then line 112 sends execution to statement 34 and G_a and G_b are calculated according to (73) and (74). Otherwise, DO loop 35 accumulates G_a and G_b of (143) and (144) in UA and UB. The purpose of the second

term on the right-hand side of (147) is to assure that the distance between the field point and the closest point on the line $\phi = \phi_K$ on the qth source segment is no less than $\frac{1}{2} c_t \Delta_q$ before DO loop 35 is entered. This distance could be as small as $r_{pq} - \frac{1}{2} \Delta_q$. DO loop 37 accumulates G_{a1} and G_{b1} of (79) and (80) in UA and UB. Lines 130 to 142 add G_{a2} and G_{b2} of (87) and (90) to UA and UB. Nested DO loops 45 and 46 put G_{ma} of (91)-(93) in GmA for $m = 4, 5, 6$. These DO loops also put G_{mb} in GmB for $m = 4, 5, 6$. The DO loop indices M and K correspond, respectively, to $(n-M+1)$ and ℓ in (91).

Lines 176 to 197 apply method 3 to G_{5a} . Expression (97) for G_{5a} consists of three terms, namely, two double sums and a double integral. Since the first term in (97) is the result of pure Gaussian quadrature, the second and third terms in (97) are attributed to method 3. At this point, however, we do not have the first term in (97), but the modification of it due to application of method 1 in lines 96 to 174. For consistency, the inner sum in the second term in (97) should be replaced by the corresponding exact integral whenever (147) is true. This corresponding exact integral is given by

$$\frac{2}{k\Delta_q} \int_{-\frac{1}{2}\Delta_q}^{\frac{1}{2}\Delta_q} \frac{dt'}{\sqrt{t'^2 + \rho_q^2 \phi_\ell^2}} = \frac{4}{k\Delta_q} \log \left[\frac{\Delta_q}{2\rho_q \phi_\ell} + \sqrt{1 + \left(\frac{\Delta_q}{2\rho_q \phi_\ell}\right)^2} \right] \quad (148)$$

Formula 200.01. of Dwight [6] was used to obtain the right-hand side of (148). The index K of DO loop 63 corresponds to ℓ in (97). Inner DO loop 65 accumulates in D7 the inner sum in the second term in (97).

Lines 188 and 189 put (148) in D7. Line 194 puts in D8 the contribution due to the second and third terms in (97). DO loop 67 adds this contribution to the modified first term in (97).

Lines 199 to 248 calculate G_{ma} and G_{mb} according to (62), (63), (64), (66) and either (65) or (94). The index L of outer DO loop 13 corresponds to ℓ' in (62) and (63). DO loop 17 puts $(e^{-jkR_{p\ell'\ell}})/(kR_{p\ell'\ell})$ in GA(K) for $\ell = K$. If, in accordance with (106),

$$c_{\phi} \rho_q > \sqrt{(\rho' - \rho_p)^2 + (z' - z_p)^2} \quad (149)$$

then (94) is used. Otherwise, (65) is used. If (149) is not true, then line 220 sends execution to statement 51. Otherwise, lines 221 to 225 put in D6 the contribution due to the second and third terms in (94). Note that the first term in (94) is the right-hand side of (65). DO loop 32 accumulates (64), (65), and (66) in U5, U6, and U7, respectively.

Inside DO loop 31, lines 262 and 263 put G_{7a} and G_{7b} of (54) and (55) in H4A and H4B, respectively. Lines 268 to 274 calculate terms in (48)-(50). U5, U6, and U7 belong in (48), U8 and U9 in (49), and UC and UD in (50). The variables K1 to K8 defined in lines 275 to 282 give the locations in Z of the matrix elements referenced in (48)-(50). See Table 2. In Table 2, p and q run from 1 to MP except where otherwise indicated. The forbidden values of p and q in Table 2 are due to (23) and (24). The contributions (48)-(51) are accounted for in lines 283 to 310. In these lines, Z(K4), Z(K6) and Z(K8) are referenced for

Table 2. Storage of matrix elements in Z.

Location in Z	Matrix Element
Z(K1)	$(Z_n^{tt})_{p-1,q-1}$ $p \neq 1, q \neq 1$
Z(K2)	$(Z_n^{tt})_{p,q-1}$ $p \neq MP, q \neq 1$
Z(K3)	$(Z_n^{tt})_{p-1,q}$ $p \neq 1, q \neq MP$
Z(K4)	$(Z_n^{tt})_{p,q}$ $p \neq MP, q \neq MP$
Z(K5)	$(Z_n^{\phi t})_{p,q-1}$ $q \neq 1$
Z(K6)	$(Z_n^{\phi t})_{p,q}$ $q \neq MP$
Z(K7)	$(Z_n^{t\phi})_{p-1,q}$ $p \neq 1$
Z(K8)	$(Z_n^{t\phi})_{p,q}$ $p \neq MP$

the first time, but the rest of the Z's are incremented. The branch statements interspersed from lines 283 to 306 are due to the forbidden values of p and q in Table 2. The seemingly muddled and repetitive nature of the Z's in lines 283 to 309 is the result of an effort to minimize the number of branch statements executed.

```

001C LISTING OF THE SUBROUTINE ZMAT
002C THE SUBROUTINE ZMAT CALLS THE FUNCTION BLOG
003 SUBROUTINE ZMAT(M1,M2,NP,NPM1,NT,RH,ZH,X,A,XT,AT,Z)
004 COMPLEX Z(1600),U1,U2,U3,U4,U5,U6,U7,U8,U9,UA,UB,G4A(10),G5A(10)
005 COMPLEX CMLX,G6A(10),G4B(10),G5B(10),G6B(10),M4A,M5A,M6A,M6B,M6C
006 COMPLEX M6B,UC,UD,GA(48),GB(48)
007 DIMENSION RH(43),ZH(43),X(48),A(48),XT(10),AT(10),RS(42),ZS(42)
008 DIMENSION D(42),DR(42),DZ(42),DM(42),C2(48),C3(48),R2(10),Z2(10)
009 DIMENSION C4(200),C5(200),C6(200),Z7(10),R7(10),Z8(10),R8(10)
010 CT=2.
011 CP=.1
012 DO 10 I=2,NP
013 I2=I-1
014 RS(I2)=.5*(RH(I)+RH(I2))
015 ZS(I2)=.5*(ZH(I)+ZH(I2))
016 D1=.5*(RH(I)-RH(I2))
017 D2=.5*(ZH(I)-ZH(I2))
018 D(I2)=SQRT(D1*D1+D2*D2)
019 DR(I2)=D1
020 DZ(I2)=D2
021 DM(I2)=D(I2)/RS(I2)
022 10 CONTINUE
023 M3=M2-M1+1
024 M4=M1-1
025 PI2=1.570796
026 DO 11 K=1,NPM1
027 PH=PI2*(X(K)+1.)
028 C2(K)=PH*PH
029 SN=SIN(.5*PH)
030 C3(K)=4.*SN*SN
031 A1=PI2*A(K)
032 D4=.5*A1*C3(K)
033 D5=A1*COS(PH)
034 D6=A1*SIN(PH)
035 M5=K
036 DO 29 M=1,M3
037 PHM=(M4+M)*PH
038 A2=COS(PHM)
039 C4(M5)=D4*A2
040 C5(M5)=D5*A2
041 C6(M5)=D6*SIN(PHM)
042 M5=M5+NPM1
043 29 CONTINUE
044 11 CONTINUE
045 NP=NP-1
046 NT=NP-1
047 N=NT+NP
048 N2N=NT*N
049 N2=N*N
050 U1=(0..5)
051 U2=(0..2.)
052 JN=-1-N
053 DO 15 JQ=1,NP
054 KQ=2
055 IF(JQ.EQ.1) KQ=1
056 IF(JQ.EQ.MP) KQ=3
057 R1=RS(JQ)
058 Z1=ZS(JQ)
059 D1=D(JQ)
060 D2=DR(JQ)

```

```

061      D3=DZ(J0)
062      D4=D2/R1
063      D5=DM(J0)
064      SV=D2/D1
065      CV=D3/D1
066      T6=CT*D1
067      T62=T6*D1
068      T62=T62*T62
069      R6=CP*R1
070      R62=R6*R6
071      DO 12 L=1,NT
072      R2(L)=R1+D2*XT(L)
073      Z2(L)=Z1+D3*XT(L)
074      12 CONTINUE
075      U3=D2*U1
076      U4=D3*U1
077      DO 16 IP=1,MP
078      R3=RS(IP)
079      Z3=ZS(IP)
080      R4=R1-R3
081      Z4=Z1-Z3
082      FM=RA*SV+Z4*CV
083      PHM=ABS(FM)
084      PH=ABS(R4*CV-Z4*SV)
085      D6=PH
086      IF(PHM.LE.D1) GO TO 26
087      D6=PHM-D1
088      D6=SORT(D6*D6+PH*PH)
089      26 IF(IP.EQ.J0) GO TO 27
090      KP=1
091      IF(T6.GT.D6) KP=2
092      IF(R6.GT.D6) KP=3
093      GO TO 28
094      27 KP=4
095      28 GO TO (41,42,41,42),KP
096      42 DO 40 L=1,NT
097      D7=R2(L)-R3
098      D8=Z2(L)-Z3
099      Z7(L)=D7*D7+D8*D8
100      R7(L)=R3+R2(L)
101      Z8(L)=.25*Z7(L)
102      R8(L)=.25*R7(L)
103      40 CONTINUE
104      Z4=R4*R4+Z4*Z4
105      R4=R3*R1
106      R5=.5*R3*SV
107      DO 33 K=1,NPMI
108      A1=C3(K)
109      RR=Z4+R4*A1
110      UA=0.
111      UB=0.
112      IF(RR.LT.T62) GO TO 34
113      DO 35 L=1,NT
114      R=SORT(Z7(L)+R7(L)*A1)
115      SN=-SIN(R)
116      CS=COS(R)
117      UC=AT(L)/R*CMPLX(CS,SN)
118      UA=UA+UC
119      UB=XT(L)*UC+UB
120      35 CONTINUE

```

```

121      GO TO 36
122 34 DO 37 L=1,N1
123      R=SQRT(Z8(L)+R8(L)*A1)
124      SN=-SIN(R)
125      CS=COS(R)
126      UC=AT(L)/R*SN+CNPLX(-SN,CS)
127      UA=UA+UC
128      UB=XT(L)+UC+UB
129 37 CONTINUE
130      A2=FM+R5*A1
131      D9=RR-A2*A2
132      R=ABS(A2)
133      D7=R-D1
134      D8=R+D1
135      D6=SQRT(D8*D8+D9)
136      R=SQRT(D7*D7+D9)
137      IF(D7.GE.0.) GO TO 38
138      A1=ALOG((D8+D6)*(-D7+R)/D9)/D1
139      GO TO 39
140 38 A1=ALOG((D8+D6)/(D7+R))/D1
141 39 UA=A1+UA
142      UB=A2*(4./(D6+R)-A1)/D1+UB
143 36 GA(K)=UA
144      GB(K)=UB
145 33 CONTINUE
146      K1=0
147      DO 45 M=1,N3
148      H4A=0.
149      H5A=0.
150      H6A=0.
151      H4B=0.
152      H5B=0.
153      H6B=0.
154      DO 46 K=1,NPHE
155      K1=K1+1
156      D6=C4(K1)
157      D7=C5(K1)
158      D8=C6(K1)
159      UA=GA(K)
160      UB=GB(K)
161      H4A=D6*UA+H4A
162      H5A=D7*UA+H5A
163      H6A=D8*UA+H6A
164      H4B=D6*UB+H4B
165      H5B=D7*UB+H5B
166      H6B=D8*UB+H6B
167 46 CONTINUE
168      G4A(M)=H4A
169      G5A(M)=H5A
170      G6A(M)=H6A
171      G4B(M)=H4B
172      G5B(M)=H5B
173      G6B(M)=H6B
174 45 CONTINUE
175      IF(KP.NE.4) GO TO 47
176      A2=D1/(P12*R1)
177      D6=2./D1
178      D8=0.
179      DO 63 K=1,NPHE
180      A1=R4*C2(K)

```

```

181      R=R4+C3(K)
182      IF(R.LT.T62) GO TO 64
183      D7=0.
184      DO 65 L=1,NT
185      D7=D7+AT(L)/SQRT(Z7(L)+A1)
186 65 CONTINUE
187      GO TO 66
188 64 A1=A2/(X(K)+1.)
189      D7=D6+ALOG(A1+SQRT(1.+A1*A1))
190 66 D8=D8+A(K)*D7
191 63 CONTINUE
192      A1=.5*A2
193      A2=1./A1
194      D8=-P[2*D8+2./R1*(BLOG(A2)+A2*BLOG(A1))]
195      DO 67 M=1,M3
196      G5A(M)=D8+G5A(M)
197 67 CONTINUE
198      GO TO 47
199 41 DO 25 M=1,M3
200      G4A(M)=0.
201      G5A(M)=0.
202      G6A(M)=0.
203      G4B(M)=0.
204      G5B(M)=0.
205      G6B(M)=0.
206 25 CONTINUE
207      DO 13 L=1,NT
208      A1=R2(L)
209      R4=A1-R3
210      Z4=Z2(L)-Z3
211      Z4=R4+R4+Z4*Z4
212      R4=R3*A1
213      DO 17 K=1,NPM1
214      R=SQRT(Z4+R4+C3(K))
215      SN=-SIN(R)
216      CS=COS(R)
217      GA(K)=CHPLX(CS,SN)/R
218 17 CONTINUE
219      D6=0.
220      IF(R62.LE.Z4) GO TO 51
221      DO 62 K=1,NPM1
222      D6=D6+A(K)/SQRT(Z4+R4+C2(K))
223 62 CONTINUE
224      Z4=3.141593/SQRT(Z4/R4)
225      D6=-P[2*D6+ALOG(Z4+SQRT(1.+Z4*Z4))/SQRT(R4)]
226 51 A1=AT(L)
227      A2=XT(L)+A1
228      K1=0
229      DO 30 M=1,M3
230      U5=0.
231      U6=0.
232      U7=0.
233      DO 32 K=1,NPM1
234      UA=GA(K)
235      K1=K1+1
236      U5=C4(K1)*UA+U5
237      U6=C5(K1)*UA+U6
238      U7=C6(K1)*UA+U7
239 32 CONTINUE
240      U6=D6+U6

```

```

241      G4A(N)=A1*U5+G4A(N)
242      G5A(N)=A1*U6+G5A(N)
243      G6A(N)=A1*U7+G6A(N)
244      G4B(N)=A2*U5+G4B(N)
245      G5B(N)=A2*U6+G5B(N)
246      G6B(N)=A2*U7+G6B(N)
247      30 CONTINUE
248      13 CONTINUE
249      47 A1=DR(IP)
250      UA=A1*U3
251      UB=DZ(IP)*U4
252      A2=D(IP)
253      D6=-A2*D2
254      D7=D1*A1
255      D8=D1*A2
256      JM=JN
257      DO 31 N=1,N3
258      FN=M4+N
259      A1=FN*DN(IP)
260      H5A=G5A(N)
261      H5B=G5B(N)
262      H4A=G4A(N)+H5A
263      H4B=G4B(N)+H5B
264      H6A=G6A(N)
265      H6B=G6B(N)
266      U7=UA+H5A+UB*H4A
267      U8=UA+H5B+UB*H4B
268      U5=U7-U8
269      U6=U7+U8
270      U7=-U1*H4A
271      U8=D6*H6A
272      U9=D6*H6B-A1*H4A
273      UC=D7*(H6A+D4*H6B)
274      UD=FM*D5*H4A
275      K1=(P+JM)
276      K2=K1+I
277      K3=K1+N
278      K4=K2+N
279      K5=K2+NT
280      K6=K4+NT
281      K7=K3+N2N
282      K8=K4+N2N
283      GO TO (18,20,19),K0
284      18 Z(K6)=U8+U9      301      Z(K6)=U8+U9
285      IF(IP.EQ.1) GO TO 21 302      IF(IP.EQ.1) GO TO 24
286      Z(K3)=Z(K3)+U6-U7 303      Z(K1)=Z(K1)+U5+U7
287      Z(K7)=Z(K7)+UC-UD 304      Z(K3)=Z(K3)+U6-U7
288      IF(IP.EQ.MP) GO TO 22 305      Z(K7)=Z(K7)+UC-UD
289      21 Z(K4)=U6+U7      306      IF(IP.EQ.MP) GO TO 22
290      Z(K8)=UC+UD      307      24 Z(K2)=Z(K2)+U5-U7
291      GO TO 22      308      Z(K4)=U6+U7
292      19 Z(K5)=Z(K5)+U8-U9 309      Z(K8)=UC+UD
293      IF(IP.EQ.1) GO TO 23 310      22 Z(K8+NT)=U2*(D8*(H5A+D4*H5B)-A1*UD)
294      Z(K1)=Z(K1)+U5+U7 311      JM=JM+N2
295      Z(K7)=Z(K7)+UC-UD 312      31 CONTINUE
296      IF(IP.EQ.MP) GO TO 22 313      16 CONTINUE
297      23 Z(K2)=Z(K2)+U5-U7 314      JN=JN+N
298      Z(K8)=UC+UD      315      15 CONTINUE
299      GO TO 22      316      RETURN
300      20 Z(K5)=Z(K5)+U8-U9 317      END

```

III. THE FUNCTION BLOG

The function BLOG(x) calculates $\log(x + \sqrt{1+x^2})$ for $x \geq 0$. If x is appreciable compared to 1, the FORTRAN supplied subroutine for the logarithm suffices. However, if x is much smaller than 1, this subroutine fails because of excessive roundoff error. From formulas 700.1. and 706. of Dwight [6],

$$\log(x + \sqrt{1+x^2}) = x(1 - \frac{1}{2 \cdot 3} x^2 + \frac{1 \cdot 3}{2 \cdot 4 \cdot 5} x^4 - \frac{1 \cdot 3 \cdot 5}{2 \cdot 4 \cdot 6 \cdot 7} x^6 + \dots), \quad x^2 < 1 \quad (150)$$

If $|x| \leq .1$, the approximation

$$\log(x + \sqrt{1+x^2}) = x(1 - \frac{x^2}{6} + \frac{3x^4}{40}) \quad (151)$$

incurs an error of less than one part in 10^7 . The function BLOG(x) uses the FORTRAN supplied subroutine for the logarithm for $x > .1$ and (151) for $x \leq .1$.

```
001C    LISTING OF THE FUNCTION BLOG
002    FUNCTION BLOG(X)
003    IF(X.GT..1) GO TO 1
004    X2=X*X
005    BLOG=(( .075*X2-.1666667)*X2+1.)*X
006    RETURN
007    1 BLCG=ALOG(X+SQRT(1.+X*X))
008    RETURN
009    END
```


IV. THE SUBROUTINE PLANE

The subroutine PLANE(M1,M2,NF,NP,NT,RH,ZH,XT,AT,THR,R) calculates the elements of the plane wave excitation vectors according to (124)-(127) and (132)-(133) and stores them in R. R is the only output argument. The rest of the arguments of PLANE are input arguments. There are NF angles of incidence θ_c of (110) and $n = M1, M1+1, \dots, M2$ where $M1 \geq 0$. The Kth angle of incidence resides in THR(K) in radians. For the first angle of incidence and for $n = M1$, storage in R is as follows.

$$\begin{aligned}
 V_{ni}^{t\theta} & \text{ in } R(i) \\
 -V_{ni}^{\phi\theta} & \text{ in } R(i+NP-2) \\
 -V_{ni}^{t\phi} & \text{ in } R(i+N) \\
 V_{ni}^{\phi\phi} & \text{ in } R(i+N+NP-2)
 \end{aligned}
 \tag{152}$$

Here,

$$N = 2*NP-3 \tag{153}$$

The minus signs are attached to $V_{ni}^{\phi\theta}$ and $V_{ni}^{t\phi}$ in (152) so that, according to (1-100) and (1-104), the vectors stored in R will be measurement vectors. For the Kth angle of incidence and for $n \geq M1$, the storage arrangement of $V_{ni}^{t\theta}$, $-V_{ni}^{\phi\theta}$, $-V_{ni}^{t\phi}$, and $V_{ni}^{\phi\phi}$ is still the same as indicated above, but the storage area now extends from $R(2*N*((K-1)*(M2-M1+1) + n-M1) + 1)$ to $R(2*N*((K-1)*(M2-M1+1) + n-M1+1))$ instead of from $R(1)$ to $R(2*N)$. Table 3 relates the fourth to ninth arguments of PLANE to variables in Part One of the text. In Table 3, $\rho(t_i^-)$ and $z(t_i^-)$ are the values of ρ and z at $t = t_i^-$ for $i = 1, 2, \dots, P$.

Table 3. Fourth to ninth arguments of PLANE

Argument of PLANE	Variable in Part One
NP	P
NT	n_T
RH	$k\rho(t_1^-), k\rho(t_2^-), \dots, k\rho(t_p^-)$
ZH	$kz(t_1^-), kz(t_2^-), \dots, kz(t_p^-)$
XT	$x_1^{(n_T)}, x_2^{(n_T)}, \dots, x_{n_T}^{(n_T)}$
AT	$A_1^{(n_T)}, A_2^{(n_T)}, \dots, A_{n_T}^{(n_T)}$

Minimum allocations are given by

COMPLEX R(2*N*NF*(M2-M1+1)), FA(M2+3), FB(M2+3)

DIMENSION RH(NP), ZH(NP), XT(NT), AT(NT),

THR(NF), CS(NF), SN(NF), R2(NT), Z2(NT)

where N is given by (153).

The index IP of DO loop 12 obtains p in (124)-(127). DO loop 13 puts $\frac{k}{2} \hat{\rho}_\ell$ of (134) and $k\hat{z}_\ell$ of (135) in R2(L) and Z2(L), respectively, for $\ell = L$. The index K of DO loop 14 obtains the Kth angle of incidence.

The index L of DO loop 15 obtains ℓ in (132) and (133). Line 48 puts $\frac{k}{2} \hat{\rho}_\ell \sin \theta_t$ in X. Lines 49 to 73 calculate S and BJ(m+2) so that

$$BJ(m+2) = S * J_m(k\hat{\rho}_\ell \sin \theta_t), \quad m = M-1, M, \dots M+1$$

$$m \neq -1$$

If the argument of the Bessel function J_m in the above equation does not exceed 10^{-7} , lines 50 to 54 use the approximations

$$J_m = \begin{cases} 0, & m \neq 0 \\ 1, & m = 0 \end{cases}$$

in order to obtain $BJ(m+2)$ and S . The purpose of lines 56 and 57 is to obtain M so large that $|J_{M-2}(k\hat{\rho}_\ell \sin \theta_t)|$ is roughly 10^{-8} . Line 58 assures that M is at least as large as $M+3$. Lines 59 to 67 start with

$$J_{M-2}(x) = 0$$

$$J_{M-3}(x) = 1$$

and use the recurrence relation

$$J_{n-1}(x) = \frac{2n}{x} J_n(x) - J_{n+1}(x)$$

taken from (9.1.27) on page 361 of [12] to calculate $J_n(x)$ for $n = M-4, M-5, \dots 0$. Lines 68 to 73 use

$$1 = J_0(x) + 2J_2(x) + 2J_4(x) + 2J_6(x) + \dots$$

taken from (9.1.46) on page 361 of [12] to obtain the normalization constant S . As the index of DO loop 15 changes, DO loop 25 accumulates F_{ma} and F_{mb} of (132) and (133) in $FA(m+2)$ and $FB(m+2)$, respectively. If $F_{-1,a}$ and $F_{-1,b}$ are needed, lines 83 and 84 use the formulas

$$F_{-1,a} = F_{1a}$$

$$F_{-1,b} = F_{1b}$$

to store $F_{-1,a}$ and $F_{-1,b}$ in FA(1) and FB(1), respectively.

With reference to (124)-(127), the index M of DO loop 27 obtains (n+2). Inside DO loop 27, UA is π_j^n . The variables U2, U3, U4, and U5 calculated in lines 95 to 98 are needed in order to assemble the right-hand sides of (124) and (126). The variables K1, K2, K4, and K5 are the subscripts of R for $V_{n,p-1}^{t\theta}$, $V_{np}^{t\theta}$, $V_{n,p-1}^{t\phi}$ and $V_{np}^{t\phi}$, respectively. Lines 102 and 103 obtain (125) and (127). The branch statement in line 104 is necessary because neither $V_{n,p-1}^{t\theta}$ nor $V_{n,p-1}^{t\phi}$ exists for p=1. In lines 105 and 106, $V_{n,p-1}^{t\theta}$ and $V_{n,p-1}^{t\phi}$ are incremented. The branch statement in line 107 is necessary because neither $V_{np}^{t\theta}$ nor $V_{np}^{t\phi}$ exists for p = NP-1. In lines 108 and 109, $V_{np}^{t\theta}$ and $V_{np}^{t\phi}$ are referenced for the first time.

```

001C LISTING OF THE SUBROUTINE PLANE
002 SUBROUTINE PLANE(M1,M2,NF,MP,NT,RH,ZH,XT,AT,THR,R)
003 COMPLEX R(240),U,U1,UA,UB,FA(10),FB(10),F2A,F2B,F1A,F1B,U2,U3,U4
004 COMPLEX U5,CMLX
005 DIMENSION RH(43),ZH(43),XT(10),AT(10),THR(3),CS(3),SN(3),R2(10)
006 DIMENSION Z2(10),BJ(50)
007 MP=MP-1
008 NT=MP-1
009 N=NT+MP
010 N2=2*N
011 DO 11 K=1,NF
012 X=THR(K)
013 CS(K)=COS(X)
014 SN(K)=SIN(X)
015 11 CONTINUE
016 U=(0.,1.)
017 U1=3.141593*U**M1
018 M3=M1+1
019 M4=M2+3
020 IF(M1.EQ.0) M3=2
021 M5=M1+2
022 M6=M2+2
023 DO 12 IP=1,MP
024 K2=IP
025 I=IP+1
026 DR=.5*(RH(I)-RH(IP))
027 DZ=.5*(ZH(I)-ZH(IP))
028 D1=SQRT(DR*DR+DZ*DZ)
029 R1=.25*(RH(I)+RH(IP))
030 Z1=.5*(ZH(I)+ZH(IP))
031 DR=.5*DR
032 DZ=DR/R1
033 DO 13 L=1,NT
034 R2(L)=R1+DR*XT(L)
035 Z2(L)=Z1+DZ*XT(L)
036 13 CONTINUE
037 DO 14 K=1,NF
038 CC=CS(K)
039 SS=SN(K)
040 D3=DR*CC
041 D4=-DZ*SS
042 D5=D1*CC
043 DO 23 M=M3,M4
044 FA(M)=0.
045 FB(M)=0.
046 23 CONTINUE
047 DO 15 L=1,NT
048 X=SS*R2(L)
049 IF(X.GT..5E-7) GO TO 19
050 DO 20 M=M3,M4
051 BJ(M)=0.
052 20 CONTINUE
053 BJ(2)=1.
054 S=1.
055 GO TO 18
056 19 M=2.8*X+14.-2./X
057 IF(X.LT..5) M=11.8+ALOG10(X)
058 IF(M.LT.M4) M=M4
059 BJ(M)=0.
060 JM=M-1

```

```

061      BJ(JM)=1.
062      DO 16 J=4,M
063      J2=JM
064      JM=JM-1
065      J1=JM-1
066      BJ(JM)=J1/X+BJ(J2)-BJ(JM+2)
067  16 CONTINUE
068      S=0.
069      IF(M.LE.4) GO TO 24
070      DO 17 J=4,M,2
071      S=S+BJ(J)
072  17 CONTINUE
073  24 S=BJ(2)+2.*S
074  18 ARG=Z2(L)*CC
075      UA=AT(L)/S*CMPLX(COS(ARG),SIN(ARG))
076      UB=XT(L)*UA
077      DO 25 M=M3,M4
078      FA(M)=BJ(M)*UA+FA(M)
079      FB(M)=BJ(M)*UB+FB(M)
080  25 CONTINUE
081  15 CONTINUE
082      IF(M1.NE.0) GO TO 26
083      FA(1)=FA(3)
084      FB(1)=FB(3)
085  26 UA=U1
086      DO 27 M=M5,M6
087      M7=M-1
088      M8=M+1
089      F2A=UA*(FA(M8)+FA(M7))
090      F2B=UA*(FB(M8)+FB(M7))
091      UB=U*UA
092      F1A=UB*(FA(M8)-FA(M7))
093      F1B=UB*(FB(M8)-FB(M7))
094      U4=D4*UA
095      U2=D3*F1A+U4*FA(M)
096      U3=D3*F1B+U4*FB(M)
097      U4=DR*F2A
098      U5=DR*F2B
099      K1=K2-1
100      K4=K1+N
101      K5=K2+N
102      R(K2+M1)=-D5*(F2A+D2*F2B)
103      R(K5+M1)=D1*(F1A+D2*F1B)
104      IF((P.EQ.1) GO TO 21
105      R(K1)=R(K1)+U2-U3
106      R(K4)=R(K4)+U4-U5
107      IF((P.EQ.NP) GO TO 22
108  21 R(K2)=U2+U3
109      R(K5)=U4+U5
110  22 K2=K2+N2
111      UA=UB
112  27 CONTINUE
113  14 CONTINUE
114  12 CONTINUE
115      RETURN
116      END

```

V. THE SUBROUTINES DECOMP AND SOLVE

The subroutines DECOMP(N, IPS, UL) and SOLVE(N, IPS, UL, B, X) solve a system of N linear equations in N unknowns. The input to DECOMP consists of N and the N by N matrix of coefficients on the left-hand side of the matrix equation stored by columns in UL. The output from DECOMP is IPS and UL. This output is fed into SOLVE. The rest of the input to SOLVE consists of N and the column of coefficients on the right-hand side of the matrix equation stored in B. SOLVE puts the solution to the matrix equation in X.

Minimum allocations are given by

COMPLEX UL(N*N)

DIMENSION SCL(N), IPS(N)

in DECOMP and by

COMPLEX UL(N*N), B(N), X(N)

DIMENSION IPS(N)

in SOLVE.

More detail concerning DECOMP and SOLVE is on pages 46-49 of [13].

```

001 C      LISTING OF THE SUBROUTINES DECOMP AND SOLVE
002      SUBROUTINE DECOMP(N,IPS,UL)
003      COMPLEX UL(1600),PIVOT,EN
004      DIMENSION SCL(40),IPS(40)
005      DO 5 I=1,N
006      IPS(I)=I
007      RN=0.
008      J1=I
009      DO 2 J=1,N
010      ULM=ABS(REAL(UL(J1)))+ABS(AIMAG(UL(J1)))
011      J1=J1+N
012      IF(RN-ULM) 1,2,2
013      1 RN=ULM
014      2 CONTINUE
015      SCL(I)=1./RN
016      5 CONTINUE
017      NM1=N-1
018      K2=0
019      DO 17 K=1,NM1
020      BIG=0.
021      DO 11 I=K,N
022      IP=IPS(I)
023      IPK=IP+K2
024      SIZE=(ABS(REAL(UL(IPK)))+ABS(AIMAG(UL(IPK))))+SCL(IP)
025      IF(SIZE-BIG) 11,11,10
026      10 BIG=SIZE
027      IPV=I
028      11 CONTINUE
029      IF(IPV-K) 14,15,14
030      14 J=IPS(K)
031      PS(K)=(PS(IPV)
032      PS(IPV)=J
033      15 KPP=(PS(K)+K2
034      PIVOT=UL(KPP)
035      KPI=K+1
036      DO 16 I=KPI,N
037      KP=KPP
038      IP=(PS(I)+K2
039      EN=-UL(IP)/PIVOT
040      18 UL(IP)=-EN
041      DO 16 J=KPI,N
042      IP=IP+N
043      KP=KP+N
044      UL(IP)=UL(IP)+EN*UL(KP)
045      16 CONTINUE
046      K2=K2+N
047      17 CONTINUE
048      RETURN
049      END
050      SUBROUTINE SOLVE(N,IPS,UL,B,X)
051      COMPLEX UL(1600),B(40),X(40),SUM
052      DIMENSION IPS(40)
053      NP1=N+1
054      IP=IPS(1)
055      X(1)=B(IP)
056      DO 2 I=2,N
057      IP=IPS(I)
058      PB=IP
059      NI=-1
060      SUM=0.
061      DO 1 J=1,NI
062      SUM=SUM+UL(IP)*X(J)
063      1 IP=IP+N
064      2 X(I)=B(IP)-SUM
065      K2=N+(N-1)
066      IP=(PS(N)+K2
067      X(N)=X(N)/UL(IP)
068      DO 4 IBACK=2,N
069      I=NP1-IBACK
070      K2=K2-N
071      IP=(IPS(I)+K2
072      IP1=I+1
073      SUM=0.
074      IP=IP1
075      DO 3 J=IP1,N
076      IP=IP+N
077      3 SUM=SUM+UL(IP)*X(J)
078      4 X(I)=(X(I)-SUM)/UL(IP1)
079      RETURN
080      END

```


VI. THE MAIN PROGRAM

The main program calculates the electric current induced by a plane wave axially incident on a perfectly conducting surface of revolution. This plane wave is given by (108) with $\theta_t = 0$ or π radians. The components of the electric current are obtained from (140) and (141) in which I_{1p}^t and I_{1p}^ϕ are the pth elements of the vectors \vec{I}_1^t and \vec{I}_1^ϕ which satisfy (6) for $n=1$.

Punched card data are read in according to

```
      READ(1,15) NT, NPHI
15    FORMAT(2I3)
      READ(1,10)(XT(K), K=1, NT)
      READ(1,10)(AT(K), K=1, NT)
10    FORMAT(5E14.7)
      READ(1,10)(X(K), K=1, NPHI)
      READ(1,10)(A(K), K=1, NPHI)
      READ(1,16) NP, BK, THR(1)
16    FORMAT(I3, 2E14.7)
      READ(1,18)(RH(I), I=1, NP)
      READ(1,18)(ZH(I), I=1, NP)
18    FORMAT(10F8.4)
```

Here, BK is the propagation constant k and ~~THR(1)~~ is the angle of incidence θ_t in radians. THR(1) must be either 0 or π . The input variables NT, NPHI, XT, AT, X, A, and NP are defined in Table 1.

These input variables can therefore be fed directly into the subroutine ZMAT. However, RH and ZH must be multiplied by BK before being fed

into ZMAT. More precisely, RH and ZH are values of ρ and z so that the product of RH with BK is the RH in Table 1, and the product of ZH with BK is the ZH in Table 1. The sample input and output data listed along with the main program are for the spherical shell of Fig. 10.

Minimum allocations are given by

```

COMPLEX Z(N*N), R(2*N), B(N), C(N)
DIMENSION RH(NP), ZH(NP), X(NPHI),
          A(NPHI), XT(NT), AT(NT), IPS(N)

```

where $N = 2*NP-3$.

With reference to (6), line 41 puts the moment matrix in Z. Line 46 puts the excitation vector \vec{V}_1^t of (6) and the negative of the excitation vector \vec{V}_1^ϕ of (6) in R(1) to R(2*NP-3). These excitation vectors are for the θ -polarized plane wave (108) and their elements are called $V_{1i}^{t\theta}$ and $V_{1i}^{\phi\theta}$. Storage in R is according to (152). Now, $-V_{1i}^{t\phi}$ and $V_{1i}^{\phi\phi}$ are also stored in R, but are not used. Lines 47 to 52 put \vec{V}_1^t and \vec{V}_1^ϕ in B. Lines 55 and 56 put the solution vectors \vec{I}_1^t and \vec{I}_1^ϕ to (6) in C. DO loop 24 prints out (140) at $\phi = 0^\circ$. DO loop 27 prints out (141) at $\phi = 90^\circ$.

```

001 C      LISTING OF THE MAIN PROGRAM
002 C      THE SUBROUTINES ZMAT, PLANE, DECOMP, AND SOLVE ARE CALLED.
003 //PGM JOB (XXXX,XXX,1,2),*MAUTZ,JOE*,REGION=200K
004 // EXEC WATFIV
005 //GO.SYSIN DD *
006 $JOB          MAUTZ.TIME=5,PAGES=60
007      COMPLEX Z(1600),R(240),B(40),C(40),U,C1
008      DIMENSION THR(3),RH(43),ZH(43),X(48),A(48),XT(10),AT(10),IPS(40)
009      READ(1,15) NT,NPHI
010      15 FORMAT(2I3)
011      WRITE(3,30) NT,NPHI
012      30 FORMAT(' NT NPHI'/(1X,13,15))
013      READ(1,10)(XT(K),K=1,NT)
014      READ(1,10)(AT(K),K=1,NT)
015      10 FORMAT(5E14,7)
016      WRITE(3,11)(XT(K),K=1,NT)
017      WRITE(3,12)(AT(K),K=1,NT)
018      11 FORMAT(' XT'/(1X,5E14,7))
019      12 FORMAT(' AT'/(1X,5E14,7))
020      READ(1,10)(X(K),K=1,NPHI)
021      READ(1,10)(A(K),K=1,NPHI)
022      WRITE(3,13)(X(K),K=1,NPHI)
023      WRITE(3,14)(A(K),K=1,NPHI)
024      13 FORMAT(' X'/(1X,5E14,7))
025      14 FORMAT(' A'/(1X,5E14,7))
026      READ(1,16) NP,BK,THR(1)
027      16 FORMAT(13,2E14,7)
028      WRITE(3,17) NP,BK,THR(1)
029      17 FORMAT(' NP',6X,'BK',12X,'THR'/(1X,13,2E14,7))
030      READ(1,18)(RH(I),I=1,NP)
031      READ(1,18)(ZH(I),I=1,NP)
032      18 FORMAT(10F8,4)
033      WRITE(3,19)(RH(I),I=1,NP)
034      WRITE(3,20)(ZH(I),I=1,NP)
035      19 FORMAT(' RH'/(1X,10F8,4))
036      20 FORMAT(' ZH'/(1X,10F8,4))
037      DO 28 J=1,NP
038      RH(J)=BK*RH(J)
039      ZH(J)=BK*ZH(J)
040      28 CONTINUE
041      CALL ZMAT(1,1, NP,NPHI,NT,RH,ZH,X,A,XT,AT,Z)
042      NT=NP-2
043      N=2*NT+1
044      WRITE(3,29)(Z(J),J=1,N)
045      29 FORMAT(' Z'/(1X,6E11,4))
046      CALL PLANE(1,1,1, NP,NT,RH,ZH,XT,AT,THR,R)
047      DO 22 J=1,NT
048      B(J)=R(J)
049      J1=J+NT
050      B(J1)=-R(J1)
051      22 CONTINUE
052      B(N)=-R(N)
053      WRITE(3,23)(B(J),J=1,N)
054      23 FORMAT(' B'/(1X,6E11,4))
055      CALL DECOMP(N,IPS,Z)
056      CALL SOLVE(N,IPS,Z,B,C)
057      U=(0.,1.)
058      WRITE(3,21)
059      21 FORMAT(' REAL JT      IMAG JT      MAG JT')
060      DO 24 J=1,NT

```

```

061      C1=2./RH(J+1)*C(J)
062      C2=CABS(C1)
063      WRITE(3,25) C1,C2
064      25 FORMAT(1X,JE11.4)
065      24 CONTINUE
066      WRITE(3,26)
067      26 FORMAT('      REAL JP      IMAG JP      MAG JP')
068      NP=NP-1
069      DO 27 J=1,MP
070      C1=4./(RH(J)+RH(J+1))*U*(J+MT)
071      C2=CABS(C1)
072      WRITE(3,25) C1,C2
073      27 CONTINUE
074      STOP
075      END

$DATA
  2  20
-0.5773503E+00 0.5773503E+00
 0.1000000E+01 0.1000000E+01
-0.9931286E+00-0.9639719E+00-0.9122344E+00-0.8391170E+00-0.7463319E+00
-0.6360537E+00-0.5108670E+00-0.3737061E+00-0.2277859E+00-0.7652652E-01
 0.7652652E-01 0.2277859E+00 0.3737061E+00 0.5108670E+00 0.6360537E+00
 0.7463319E+00 0.8391170E+00 0.9122344E+00 0.9639719E+00 0.9931286E+00
 0.1761401E-01 0.4060143E-01 0.6267205E-01 0.8327674E-01 0.1019301E+00
 0.1181945E+00 0.1316886E+00 0.1420961E+00 0.1491730E+00 0.1527534E+00
 0.1527534E+00 0.1491730E+00 0.1420961E+00 0.1316886E+00 0.1181945E+00
 0.1019301E+00 0.8327674E-01 0.6267205E-01 0.4060143E-01 0.1761401E-01
 11 0.1256637E+01 0.0000000E+00
 0.0000 0.2334 0.4540 0.6494 0.8090 0.9239 0.9877 0.9969 0.9511 0.8526
 0.7071
-1.0000 -0.9724 -0.8910 -0.7604 -0.5878 -0.3827 -0.1564 0.0785 0.3090 0.5225
 0.7071

$STOP
/*
//
PRINTED OUTPUT
NT NPHE
  2  20
XT
-C.5773503E+00 0.5773503E+00
AT
 0.1000000E+01 0.1000000E+01
X
-0.9931286E+00-0.9639719E+00-0.9122344E+00-0.8391170E+00-0.7463319E+00
-0.6360537E+00-0.5108670E+00-0.3737061E+00-0.2277859E+00-0.7652652E-01
 0.7652652E-01 0.2277859E+00 0.3737061E+00 0.5108670E+00 0.6360537E+00
 0.7463319E+00 0.8391170E+00 0.9122344E+00 0.9639719E+00 0.9931286E+00
A
 0.1761401E-01 0.4060143E-01 0.6267208E-01 0.8327675E-01 0.1019301E+00
 0.1181945E+00 0.1316886E+00 0.1420961E+00 0.1491730E+00 0.1527534E+00
 0.1527534E+00 0.1491730E+00 0.1420961E+00 0.1316886E+00 0.1181945E+00
 0.1019301E+00 0.8327675E-01 0.6267208E-01 0.4060143E-01 0.1761401E-01
NP      BK      THR
11 0.1256637E+01 0.0000000E+00
RH
 0.0000 0.2334 0.4540 0.6494 0.8090 0.9239 0.9877 0.9969 0.9511 0.8526
 0.7071
ZH
-1.0000 -0.9724 -0.8910 -0.7604 -0.5878 -0.3827 -0.1564 0.0785 0.3090 0.5225
 0.7071

```

Z

0.8363E-01-0.9778E+01 0.7552E-01 0.2574E+01 0.6344E-01 0.7723E+00
0.4919E-01 0.2893E+00 0.3460E-01 0.1491E+00 0.2126E-01 0.9127E-01
0.1024E-01 0.6477E-01 0.1954E-02 0.5293E-01-0.3673E-02 0.4842E-01
-0.1348E+02 0.8701E-01 0.2413E+01 0.8414E-01 0.4250E+00 0.7858E-01
0.1369E+00 0.7103E-01 0.7633E-01 0.6213E-01 0.5943E-01 0.5265E-01
0.5437E-01 0.4326E-01 0.5275E-01 0.3455E-01 0.5202E-01 0.2694E-01
0.5134E-01 0.2063E-01

B

0.3151E+00-0.8385E+00 0.3631E+00-0.7352E+00 0.4046E+00-0.5696E+00
0.3966E+00-0.3656E+00 0.3074E+00-0.1689E+00 0.1384E+00-0.3786E-01
-0.7037E-01-0.1748E-01-0.2587E+00-0.1152E+00-0.3766E+00-0.2963E+00
0.8755E+00 0.3070E+00 0.8527E+00 0.3660E+00 0.7959E+00 0.4749E+00
0.6917E+00 0.6161E+00 0.5279E+00 0.7602E+00 0.3060E+00 0.8730E+00
0.4503E-01 0.6236E+00-0.2219E+00 0.8975E+00-0.4598E+00 0.8031E+00
-0.6438E+00 0.6653E+00

REAL JT	IMAG JT	MAG JT
0.1142E+01	0.1198E+01	0.1655E+01
0.8187E+00	0.1199E+01	0.1451E+01
0.3432E+00	0.1163E+01	0.1212E+01
-0.2206E+00	0.1035E+01	0.1058E+01
-0.7768E+00	0.7827E+00	0.1103E+01
-0.1222E+01	0.4161E+00	0.1291E+01
-0.1474E+01-0.6146E-02		0.1474E+01
-0.1489E+01-0.3877E+00		0.1538E+01
-0.1248E+01-0.6133E+00		0.1391E+01
REAL JP	IMAG JP	MAG JP
-0.1209E+01-0.1184E+01		0.1692E+01
-0.1076E+01-0.1094E+01		0.1534E+01
-0.9486E+00-0.9418E+00		0.1337E+01
-0.8584E+00-0.7213E+00		0.1121E+01
-0.8928E+00-0.4863E+00		0.1017E+01
-0.1102E+01-0.3341E+00		0.1152E+01
-0.1480E+01-0.3804E+00		0.1520E+01
-0.2002E+01-0.7355E+00		0.2133E+01
-0.2629E+01-0.1433E+01		0.2995E+01
-0.6381E+01-0.5179E+01		0.8219E+01

REFERENCES

- [1] J. R. Mautz and R. F. Harrington, "H-Field, E-Field, and Combined Field Solutions for Bodies of Revolution," Report RADC-TR-77-109, N.T.I.S. No. ADA 040379, Rome Air Development Center, Griffiss Air Force Base, N.Y., June 1977, A040379.
- [2] A. W. Glisson and D. R. Wilton, "Simple and Efficient Numerical Techniques for Treating Bodies of Revolution," Report RADC-TR-79-22, N.T.I.S. No. ADA 067361, Rome Air Development Center, Griffiss Air Force Base, New York, March 1979, A067361.
- [3] P. J. Davis and P. Rabinowitz, Methods of Numerical Integration, Academic Press, 1975, p. 139.
- [4] J. Meixner, "The Behavior of Electromagnetic Fields at Edges," IEEE Trans. Antennas Propagat., vol. AP-20, No. 4, pp. 442-446. July 1972.
- [5] V. I. Krylov, Approximate Calculation of Integrals, translated by A. H. Stroud, Macmillan Co., New York, 1962.
- [6] H. B. Dwight, Tables of Integrals and Other Mathematical Data, Macmillan, New York, 1961.
- [7] C. Cha and R. F. Harrington, "Electromagnetic Transmission through an Annular Aperture in an Infinite Conducting Screen," S.U. Report TR-79-11, N.T.I.S. No. ADA 074831, Department of Electrical and Computer Engineering, Syracuse University, Syracuse, NY. Sept. 1979.
- [8] R. F. Harrington and J. R. Mautz, "Radiation and Scattering from Bodies of Revolution," Report AFCRL-69-0305, N.T.I.S. No. AD 859670, Contract No. F-19628-67-C-0233 between Syracuse University and Air Force Cambridge Research Laboratories, July 1969.
- [9] A. J. Poggio and E. K. Miller, "Integral Equation Solutions of Three-dimensional Scattering Problems," Chapt. 4 of Computer Techniques for Electromagnetics, edited by R. Mittra, Pergamon Press, 1973.
- [10] W. A. Davis and R. Mittra, "A New Approach to the Thin Scatterer Problem Using the Hybrid Equations," IEEE Trans. Antennas Propagation, vol. AP-25, No. 3, pp. 402-406, May 1977.
- [11] C. J. Bouwkamp, "On the Diffraction of Electromagnetic Waves by Small Circular Disks and Holes," Philips Res. Rep., vol. 5, pp. 401-422, December 1950.

- [12] M. Abramowitz and I. A. Stegun, "Handbook of Mathematical Functions," U.S. Government Printing Office, Washington, D.C. (Natl. Bur. Std. U.S. Applied Math. Ser. 55), 1964.
- [13] J. R. Mautz and R. F. Harrington, "Transmission from a Rectangular Waveguide into Half Space Through a Rectangular Aperture," Interim Technical Report RADC-TR-76-264, N.T.I.S. No. ADA 030779, Rome Air Development Center, Griffiss Air Force Base, New York, August 1976, A030779.